

Path Integral Formulation of Quantum Tunneling:
Numerical Approximation and Application to
Coupled Domain Wall Pinning

Matthew Ambrose

Supervisor: Prof Robert Stamps

Honours Thesis submitted as part of the B.Sc. (Honours) degree
in the School of Physics, University of Western Australia

Date of submission: 24/October/08

Acknowledgments

Many thanks to my supervisor Bob for all his support, teaching me all that he has and generally helping give me direction in my research. Also thanks to those in the condensed matter group who have given a great deal of assistance, in particular Karen Livesy who gave a great deal of her time to proof read the thesis

A thanks is also extended to my family and friends who have been incredibly supportive.

Abstract

In this thesis we investigate numerically the macroscopic tunneling rates of a coupled system of fronts. We show that it is possible to make a new numerical approximation to the symmetric double well potential that agrees with the analytic expression for the ground state energy level splitting. Using this numerical method we then make the appropriate changes to the ground state energy calculation to treat a non symmetric potential. The introduction of an imaginary part to the ground state energy causes a decay away from the metastable side of the potential. We then treat a system that can decay from a metastable state into more than one lower energy configuration. As an example of such a system we consider a multiferroic system in which the magnetic and electric polarisations are coupled. We then proceeded to compute the tunneling rate numerically and compare the behavior of the tunneling rates for the two possible final states.

Contents

1	Introduction	1
1.1	Multiferroic Materials	2
2	Path Integrals and Quantum Tunnelling	4
2.1	The path integral formulation of quantum mechanics	4
2.2	Tunnelling in the Low Temperature Limit: The Wick Rotation	7
2.3	Feynman-Kac Formula	9
2.4	Evaluating the Integral	10
2.4.1	General Explanation of Evaluation	10
2.4.2	Instatons	11
2.4.3	Evaluating the infinite product	14
2.4.4	Zero Eigenvalue Solution	14
2.4.5	Key Results of the Double Well potential	15
2.4.6	Fluctuation contribution to Feynman Kernel	16
3	Numerical Treatment of Double Well Potential	19
3.1	Finding the Stationary Path	19
3.1.1	Classical contribution	21
3.2	Discrete Eigenvalue Contribution	21
3.3	Continuum Eigenvalue Contribution	22
3.3.1	Level Splitting formula	24
4	Metastable States	26
4.1	Semi-Classical Tunnelling Formula	28
5	Application to Multiferroic System	30
5.1	Representation of The Domain walls	30
5.1.1	Magnetic Domain Walls	30
5.1.2	Polarization Domain Walls	31
5.1.3	Width Dependence of Energy	32
5.2	Driving Force, Defect and Coupling	32

5.3	Domain Wall Inertia	33
5.3.1	Euler Lagrange Equations	34
5.4	Determining the End Points: Multiple Solutions	34
5.5	Varying the applied field	36
5.6	Varying the coupling strength	37
6	Conclusion	39
	References	42
A	Analytic Treatment of Double Well Potential	43
A.1	General Explanation of Evaluation	43
A.1.1	Evaluating the infinite product	46
A.1.2	Zero Eigenvalue Solution	47
A.2	Specifics of Double Well potential	47
A.2.1	Classical Contribution to the Action	48
A.2.2	Fluctuation contribution to Feynman Kernal	48
A.3	Descrete Eigen Value Contribution	48
A.4	Continum Eigenvalue Contribution	49
A.5	Rare Gas of Instatons	53

Chapter 1

Introduction

If the finite characteristic lifetime of a state is greater than the timescales of other processes in a system we say that such a state is metastable. Metastable states and the processes by which they relax are responsible for phenomena as diverse as the lifetime of excited states in atoms to the behavior of super cooled gases. Typically for macroscopic systems one considers the mechanism for decay of metastable states to be via stochastic processes in which the decay occurs through energy exchange mediated by a coupling with the environment[6].

More recently the concept of so called macroscopic quantum tunneling has been considered as a mechanism for systems to enter into equilibrium. In 1959 Goldanskii showed, that at sufficiently low temperature, quantum tunnelling is the dominant mechanism for decay and it has become possible to construct experiments in which tunneling of macroscopic parameters occur.

We will be interested in analysing the behavior of a system where there are two possible final states that the system might tunnel into. For these systems the form of the potential energy is complicated and employing Schrödinger wave mechanics would usually represent an incredibly difficult task. In analysing these tunneling problems it is particularly convenient to employ Feynman's path integral representation of quantum mechanics [3, 6]. In this formalism it is necessary only to form a Lagrangian of the macroscopic variables that describe the system in order to analyse tunneling from a metastable configuration. While it might seem inconsistent to treat macroscopic quantities in an essentially quantum mechanical frame work, if the system is at sufficiently low energies the underlying quantum structure is not apparent and our treatment will be acceptable.

A direct example of this concept could be found in an alpha particle. At low energies we can consider a point particle and describe it by only position and momentum, at higher energies one would need to consider the particle as four interacting particles (two protons and two neutrons) and at even greater energies still we would have to consider the structure in terms of quarks. In order for macroscopic tunneling to be prevalent we do require that the effective mass of the parameter that we are treating be sufficiently small.

1.1 Multiferroic Materials

A real system to which our proposed numerical evaluation can be applied is a multiferroic system which exhibits both spontaneous ferromagnetic and ferroelectric ordering. A pure ferroelectric material is one which exhibits a spontaneous polarization. For such a material there exists a static energy[14].

$$E_D = \frac{1}{2} \int_{\text{Vol}} dV \vec{D} \cdot \vec{E} \quad (1.1)$$

In real crystals the effects at the surface and at defects in the crystal lattice will cause the system to form regions of oppositely oriented polarization in the absence of an applied electric field. Similarly ferromagnetic materials are those that exhibit a spontaneous magnetic ordering. In order to minimise the magnetostatic energy [11]

$$E_D = \frac{1}{8\pi} \int_{\text{Vol}} dV \vec{B} \cdot \vec{B}, \quad (1.2)$$

these materials also form regions of uniform order. In both cases we refer to the regions of uniform order as domains and the boundary between regions as domain walls. In the model presented in the 5th chapter we will consider magnetic domain walls where the magnetization rotates perpendicular to the domain walls. For the electric domain walls will correspond to a continuous change in the magnitude of the polarization vector. The two walls are shown in figure (1.1)

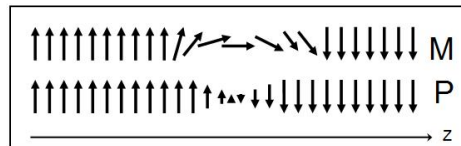


Figure 1.1: The polarization change for the magnetic and electric systems

In 2002 the correlation of electric and magnetic domain walls was observed for the first time in YMnO_3 [4]. We will model a multiferroic in which there is a symmetric energy term associated with the angle between the magnetisation and the

polarisation that acts to create an attractive force between polarization and magnetization domain walls. We will then consider the case in which the system is driven by an external electric field and introduce a planar defect that inhibits the propagation of the magnetic domain wall and hence the coupled system. And shall calculate under which conditions both walls are likely to tunnel and under which conditions only the electric domain wall is able to tunnel. Multiferroic materials are a group of compounds of great interest in condensed matter physics ([7]). They are characterised by the fact that they display spontaneous ordering both magnetically and electrically and are said to exhibit both ferroelectric and ferromagnetic properties. Of particular importance are ferroelectromagnets, substances in which the magnetization can be induced by an electric field (and) or the polarisation can be induced by a magnetic field. Aside from fundamental interest, there exists the possibility to utilise them in storage media as four state memories.

Before describing the multiferroic system in greater detail we will present some of the key structure of the Feynman treatment. We will show a new method by which the important integrals of the theory can be evaluated numerically and compare the results with a known analytic solution. We will then derive a set Euler Lagrange equations for the multiferroic system described above and investigate various behaviours of the system.

Chapter 2

Path Integrals and Quantum Tunnelling

2.1 The path integral formulation of quantum mechanics

We begin by introducing the path integral formulation of quantum mechanics. The functional integral formulation of quantum mechanics was first suggested by Richard Feynman in 1948 in [3] and it is his explanation closely followed here. One might feel that this presentation of the path integral is not entirely satisfactory. Several important issues will not have been addressed. There are other direct and rigorous proofs, where the path integral is derived by considering only the initial and final states and a limiting process involving an infinite process of time evolution operators, such a proof is presented in the book [12]. Here we do not aim to provide a proof but rather an explanation of the key concepts. This presentation gives an intuitive feel, by motivating a probability like amplitude associated with paths, that can be obscured in other presentations.

We begin with a review of probability in the quantum and classical regimes. Let P_{ac} be the probability that given some measurement A gives a result a that a measurement of C gives result c , for clarity it is useful to imagine A and C to be repeated position measurements of a particle in one dimension (C must be made at time $t_a < t_c$). If we now make an additional measurement B at a time between measurements of A and C we have the result that the probability of being at a and then b and then c is the product of the probability of being at b given that the particle was a a with the probability of being at c given that the particle was a b or much more succinctly,

$$(2.1) \quad P_{abc} = P_{ab}P_{bc}.$$

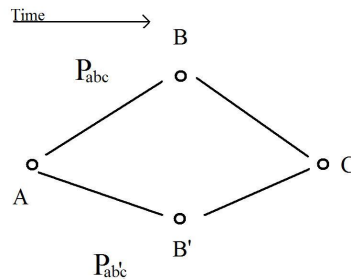


Figure 2.1: In this idealised situation we assume that a point particle starts at A and we wish to find the probability that at some fixed time later the particle arrives at position C . At some interim time we make an assumption that the particle could be in one of only two positions B or B'

In figure 2.1 we now consider that at some interim time the particle is now allowed to take a discrete number of possible values (in the case of the figure only two values). Since probability is additive we have in the probability of finding the particle at C to be,

$$P_{ac} = \sum_b P_{abc} \quad (2.2)$$

where the sum is over all possible allowed values for measurement B . We would say that P_{abc} contribution to the likelihood of measuring c when the particle was initially at some position a later at some position b and then at some position c . So far we have not encountered anything unfamiliar. Quantum mechanically, however, we must consider the effect of not making the measurement b . Classically this sentence does not make sense, the particle assumes some value for measurement of b regardless of observation. The amazing result of quantum mechanics is that when measurement B is not performed equation 2.2 is generally incorrect. We have instead the quantum mechanical law

$$\varphi_{ac} = \sum_b \varphi_{ab}\varphi_{bc} \quad (2.3)$$

where φ are complex numbers and it is the norm of these complex numbers (often called probability amplitudes) that give a probability. This difference is subtle but its implications are of great importance. The distinguishing property is that the probability amplitudes carry an amplitude and a phase allowing for interference

effects in our probability amplitudes. This is of great importance and is key to understanding the path integral formulation. Before continuing a few comments are in order:

1. In equations (2.2) and (2.3) the summation implied a discrete set of allowed values for measurement B in general the allowed values will be continuous and unbounded, hence summation will be replaced by an integral.

2. In the quantum mechanical formula (2.3) the allowed values are not limited to those allowed in equation (2.2). When we are measuring B we are restrained to measure values that are physically meaningful b , in the absence of this measurement we are not. One consequence of this is that if during the interim time there existed a potential barrier so that for all b $V(b) > E$ where E is the energy of our particle the probability of measuring c is non-zero. We label this non-zero probability as the quantum tunnelling probability, since a particle will have moved from one classically allowed state to another through a classically forbidden region.

To continue we consider the time evolution amplitude $\langle x_b | \widehat{U}(t_b, t_a) | x_a \rangle$, where \widehat{U} is the time evolution operator. Let the time interval be sliced into N parts and indexed t_n with $n = 0, 1, 2, \dots, N$ and the possible values of the position of the particle at time t_n labeled x_n . Remembering that the summation has been replaced with an integral we could write our probability amplitude as:

$$\langle x_b | \widehat{U}(t_b, t_a) | x_a \rangle = \int_{-\infty}^{\infty} dx_0 \int_{-\infty}^{\infty} dx_1 \dots \int_{-\infty}^{\infty} dx_N \prod \varphi_{x_n x_{n+1}} \quad (2.4)$$

where the product is over all $n = 0, 1, 2, \dots, N$. Noting that the product is dependent only the values of our x_n define a complex valued function

$$\Phi(\dots x_i, x_{i+1}, \dots) = \prod \varphi_{x_n x_{n+1}}, \quad (2.5)$$

we can interpret $\Phi(\dots x_i, x_{i+1}, \dots)$ as the probability amplitude that a particle moves from x_a to x_b via $x_1, \dots, x_i, x_{i+1}, \dots$. Now if we increase N the spacing between points $\epsilon = \frac{1}{N}(t_b - t_a)$ will approach zero and the x_n approach a continuum, defining a smooth path. In the limit of $\epsilon \rightarrow 0$ we write $\Phi(\dots x_i, x_{i+1}, \dots) = \Phi[x(t)]$ which Feynman called the probability amplitude functional. By direct extension of our discrete function we interpret this to be the probability amplitude that a particle moves from x_a to x_b along path $x(t)$. This brings us to our definition of the path integral

$$\lim_{\epsilon \rightarrow 0} \int_{-\infty}^{\infty} dx_0 \int_{-\infty}^{\infty} dx_1 \dots \int_{-\infty}^{\infty} dx_N \Phi(\dots x_i, x_{i+1}, \dots) = \int \mathcal{D}[x(t)] \Phi[x(t)]. \quad (2.6)$$

We have now that time evolution amplitude $\langle x_b | \widehat{U}(t_b, t_a) | x_a \rangle$ is the sum of complex contributions from each path between the end points. All that remains is to evaluate $\Phi[x(t)]$ for each path, to do this we introduce the postulate according to Feynman:

The paths contribute equally in magnitude, but the phase of their contribution is the classical action; the time integral of the Lagrangian of the path

$$\int \mathcal{D}[x(t)] e^{\frac{i}{\hbar} S[x(t)]}. \quad (2.7)$$

It might seem that the probability amplitude association with each path is lost by allowing $\|\Phi[x(t)]\|$ to be constant, however, the varying phase allows for paths to interfere with one another. It might seem that the appearance of the classical action is not well motivated; it is not necessary to introduce the classical action at this point. We could have introduced an arbitrary functional and then required that in the high mass limit classical paths be the dominant contributions to the path. Recalling that for a standard integral of the same form we would require that the exponent have at least one stationary point to be non-zero. It is not hard to imagine in direct analogue that stationary paths of the functional will give us our dominant contribution. Hence in the high mass limited we need a functional whose stationary points are the paths taken in classical mechanics.

We now have a formulation of quantum mechanics that requires only the formulation of a suitable Lagrangian and not the use of the equivalence principal to create operators. It can be shown that this formulation is completely equivalent, it is possible to derive the wave mechanics and matrix formulations directly from the path integral formulation [3]. This approach has proved crucial in the calculations of quantum field theory and can be easily extended for calculations in statistical physics.

2.2 Tunnelling in the Low Temperature Limit: The Wick Rotation

In order to treat situations of metastability it will be necessary to consider how one could treat the situation of quantum tunnelling in the path integral formalism. Consider the simple one dimensional potential given by 2.2, we will label the two minima x_i and x_f referring to the metastable and stable configurations respectively,

we also label the height of the barrier V_0 . Now consider the Feynman propagator determining the probability that the system is found in configuration x_i at time t_i and then at x_f and at time t_f .

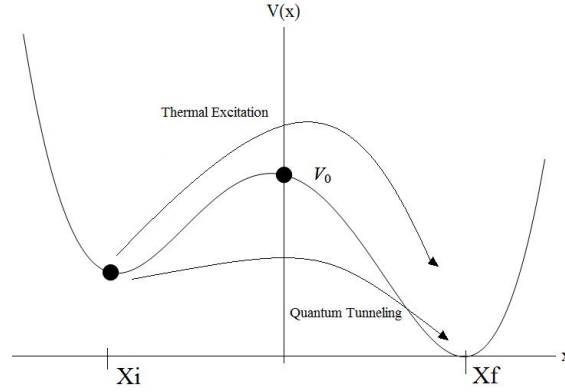


Figure 2.2: This potential has a local minimum that is rendered metastable by either tunneling or thermal excitation

$$\langle x_f | e^{-\frac{i\hat{H}t}{\hbar}} | x_i \rangle = \int \mathcal{D}[x(t)] e^{-\frac{iS}{\hbar}} \quad (2.8)$$

with

$$S = \frac{m}{2} \int_0^t dt \left(\frac{dx}{dt} \right)^2 - V(x)$$

In order to approximate this path integral one would normally attempt to find a path that was stationary with respect to S . Since this path will provide the dominant contribution to the integral one could make an expansion of the action around this path. Further explanation of exactly how this is done is given below in section 2.4.2. However, in the case of the total energy of the system being less than V_0 we know that there cannot exist such a stationary path (if we were able to find one it would correspond to a classical path from x_i to x_f). We could, however, treat the system using the Schrödinger wave mechanics formulation where we would expect energy eigensolutions to the time independent Schrödinger equation to exhibit exponential behavior “inside” the barrier. In order to continue we perform the so called Wick rotation $t \rightarrow i\tau$. In the appendix we show that this transformation essentially has the effect of inverting the potential in the action. Mathematically we are now able to make some progress in evaluating the integral since a stationary path is at least in theory now obtainable. We are however left with the problem of how to interpret

our transformed propagator.

$$\langle x_f | e^{\frac{-\hat{H}\tau}{\hbar}} | x_i \rangle = \int \mathcal{D}[x(\tau)] e^{\frac{-S_e}{\hbar}} \quad (2.9)$$

with

$$S_e = \frac{m}{2} \int_{-\frac{\tau}{2}}^{\frac{\tau}{2}} d\tau \left(\frac{d}{d\tau} x \right)^2 + V(x).$$

Recall that the quantum statistical partition function may be viewed as an analytic continuation of the quantum mechanical partition function. then we can write the Quantum statistical Partition function as

$$Z = \int_{-\infty}^{\infty} dx \langle x | e^{\frac{-i\hat{H}t}{\hbar}} | x \rangle \Big|_{t_f - t_i \rightarrow -i\hbar\beta} \quad (2.10)$$

If it were the case that there were only a single x with a closed stationary path associated with it one could omit the trace integral and approximate the partition function by

$$Z = \int \mathcal{D}[x(\tau)] e^{\frac{-S_e}{\hbar}} \quad (2.11)$$

where we have substituted the expression for the transformed propagator. We see that our transformed propagator has the form of a partition function. Despite this, in chapter 4 we will calculate the above expression for a state away from equilibrium and will find that we calculate a small imaginary part which relates to the rate at which the system tunnels from a metastable state.

2.3 Feynman-Kac Formula

In the low temperature limit it is possible to obtain an approximation to the ground state energy of a system using the transformed propagator. This result is used in the calculation of the ground state energy in the double well potential and will be important in the interpretation of the imaginary part appearing in the transformed propagator. To begin suppose that we have a complete set of energy eigenstates,

$$\hat{H}|\varphi_n\rangle = E_n|\varphi_n\rangle. \quad (2.12)$$

Then we can write the propagator in terms of a complete set of energy eigenfunctions, resulting in the so called spectral decomposition:

$$G(x_f, t; x_i, 0) = \langle x_f | \hat{U}(t) | x_i \rangle = \sum_{n=0}^{\infty} \langle x_f | \varphi_n \rangle \langle \varphi_n | e^{\frac{i\hat{H}t}{\hbar}} | x_i \rangle = \sum_{n=0}^{\infty} \varphi_n(x_f) e^{\frac{iE_n t}{\hbar}} \varphi_n^*(x_i). \quad (2.13)$$

Now if we set x_f to x_i and then integrate over all x we have the result, using the fact that energy eigenfunctions are orthonormal,

$$\int dx G(x_f, t; x_i, 0) = \sum_{n=0}^{\infty} e^{\frac{-iE_n t}{\hbar}} \quad (2.14)$$

We now consider the complex t behavior of the above relation with $it = \tau$ we see that as τ approaches infinity that the leading contribution will come from the ground state energy, giving the Feynman-Kac formula.

$$\int dx G(x_f, t; x_i, 0) \approx e^{\frac{-E_0 \tau}{\hbar}} \quad (2.15)$$

The above formula is usually presented rearranged for E_0 but current presentation will be more suitable for the our purposes here.

2.4 Evaluating the Integral

Having derived the Feynman-Kac formula for the ground state energy level we will consider the actual evaluation of the Wick rotated integral of equation (2.9), in particular a semi-classical approximation. At the end of this section we will give some of the key results of the analytic solution to a symmetric quartic potential in particular the level splitting formula. The full calculation with the exception of the evaluation of the Rosen Morse potential are included in the appendix. Calculation of the symmetric double well, while not an example of a metastable system, illustrates all the important aspects of calculations in the semi-classical approximation, including the ‘rare gas’ treatment of the multiple instanton solutions. We use the general results of this section in the explanation of the semi-classical tunnelling formula in chapter 4. In chapter 3 the results from the following calculation can be compared to those of the numerical approximation.

2.4.1 General Explanation of Evaluation

We begin by considering an arbitrary potential $V(x)$. As discussed, we are interested in the analytically continued $t \rightarrow i\tau$ propagator

$$\langle x_f | e^{\frac{-\hat{H}\tau}{\hbar}} | x_i \rangle, \quad (2.16)$$

in particular the leading terms in large τ regime. So we wish to evaluate

$$\langle x_f | e^{\frac{-i\hat{H}t}{\hbar}} | x_i \rangle = \int \mathcal{D}[x(t)] e^{\frac{-iS}{\hbar}} \quad (2.17)$$

with

$$S = \frac{m}{2} \int_0^t dt \left(\frac{d}{dt} x \right)^2 - V(x)$$

taking $t \rightarrow i\tau$ gives a new expression for the action

$$\begin{aligned} S &= \frac{m}{2} \int_{-\frac{\tau}{2}}^{\frac{\tau}{2}} \left(\frac{dt}{d\tau} d\tau \right) \left(\frac{d\tau}{dt} \frac{d}{d\tau} x \right)^2 - V(x) \\ &= -i \frac{m}{2} \int_{-\frac{\tau}{2}}^{\frac{\tau}{2}} d\tau i^2 \left(\frac{d}{d\tau} x \right)^2 - V(x) \end{aligned} \quad (2.18)$$

and hence we have (with the transformed action denoted S_e and referred to as the euclidean propagator)

$$\langle x_f | e^{-\frac{\hat{H}\tau}{\hbar}} | x_i \rangle = \int \mathcal{D}[x(\tau)] e^{-\frac{S_e}{\hbar}} \quad (2.19)$$

with

$$S_e = \frac{m}{2} \int_{-\frac{\tau}{2}}^{\frac{\tau}{2}} d\tau \left(\frac{d}{d\tau} x \right)^2 + V(x),$$

Note that finding the stationary points of this transformed propagator is mathematically equivalent to solving the Euler-Lagrange equations in the inverted potential $-V(x)$. We have to solve the path integral of 2.19. Exact solutions are not typically available, indeed this is the case here. We must therefore make the so called semi-classical approximation. We expand our paths in terms of weak variations around paths that are stationary with respect to the euclidean action.

2.4.2 Instatons

So far we have referred briefly to stationary paths without giving an explicit definition. For any functional we are able to make the expansion [5]

$$\begin{aligned} S_e[x(\tau)] & \\ &= S_e[\bar{x}(\tau) + \Delta x(\tau)] \\ &= S_e[\bar{x}(\tau)] + \int \frac{\delta S_e[\bar{x}(\tau)]}{\delta x(\tau)} \Delta x(t) d\tau \\ &+ \frac{1}{2!} \int \int \frac{\delta^2 S_e}{\delta x(\tau_1) \delta x(\tau_2)} \Delta x(t_1) \Delta x(t_2) d\tau_1 d\tau_2 + O\left(\frac{1}{3!} \Delta x(\tau)^3\right) \end{aligned} \quad (2.20)$$

when referring to the stationary path, denoted *overline* $x(\tau)$, we will mean the path over which the first variation is zero ($\frac{\delta S_e[\bar{x}(\tau)]}{\delta x(\tau)} = 0$). An important but not immediately obvious, result is that in the case when the action S_e is of the form in equation 2.8 and $x(\tau)$ is the stationary solution then the derivative of this solution $\dot{x}(\tau)$ will satisfy $\delta^2 S_e[\dot{x}(\tau)] = 0$. We assume currently that there is only one such path, this

is of course not generally true but we can always sum the contributions from other such stationary paths. We express any path $x(t)$ as a sum $x(t) = \overline{x(\tau)} + \Delta x(\tau)$ with $\overline{x(\tau)}$ the stationary point of the euclidean action. This stationary point is mathematically similar to the localised functions describing particles in wave mechanics and is referred to as either a pseudo-particle or an instanton, I will adopt the convention of referring to it as the instanton solution. In the situations that we are interested in (quantum tunnelling through a barrier), this solution will take the form of an essentially constant solution with a well localised change, referred to usually as either a bubble or kink (depending on whether the path returns to its original constant value or different one). The condition that the first functional derivative be zero for $\overline{x(\tau)}$ implies that $\overline{x(\tau)}$ will obey the familiar Euler-Lagrange equations, albeit for the inverted potential.

To find expressions for the terms of the expansion note that the second functional derivative of the euclidean action is

$$\frac{\delta^2 S_e}{\delta x(\tau_1) \delta x(\tau_2)} = -m \left(\frac{d^2}{d\tau^2} \delta(\tau - \tau_2) \right) \Big|_{\tau \rightarrow \tau_1} + \frac{d^2}{dx^2} V(x) \delta(\tau_1 - \tau_2). \quad (2.21)$$

So the second variation is

$$\begin{aligned} \delta^2 S_e &= \frac{1}{2!} \int \int \frac{\delta^2 S_e[\overline{x(\tau)}]}{\delta x(\tau_1) \delta x(\tau_2)} \Delta x(t_1) \Delta x(t_2) d\tau_1 d\tau_2 \\ &= \frac{m}{2} \int -\Delta x(\tau_1) \Delta x''(\tau_1) + \frac{d^2}{dx^2} V(\overline{x}(\tau_1)) \Delta x(\tau_1)^2 d\tau_1 \end{aligned} \quad (2.22)$$

the negative of the above expression is usually denoted S_e^{fl} . If the series expansion is truncated after the second order term we have

$$\begin{aligned} \langle x_f | e^{\frac{-\hat{H}\tau}{\hbar}} | x_i \rangle &= \int \mathcal{D}[x(\tau)] e^{\frac{-S_e[x(\tau)]}{\hbar}} \\ &= \int \mathcal{D}[\overline{x}(\tau) + \Delta x(\tau)] e^{\frac{-S_e[\overline{x}(\tau) + \Delta x(\tau)]}{\hbar}} \\ &\approx e^{S_e[\overline{x}(\tau)]} \int \mathcal{D}[\Delta x(\tau)] e^{\frac{-S_e^{fl}[\Delta x(\tau)]}{\hbar}} \end{aligned} \quad (2.23)$$

we usually write

$$\approx e^{\frac{-S_e[\overline{x}(\tau)]}{\hbar}} \mathcal{F}.$$

This truncation is referred to as the semi-classical approximation, we are only considering quantum effects to first order. In doing so we have factored the problem into the contribution from the instanton path and the contribution from quadratic fluctuations around that path (\mathcal{F}). Once the instanton $x(\tau)$ has been calculated, \mathcal{F} is

comparatively easy to evaluate compared to the original integral. It is quadratic in the path variations which have vanishing end points. To proceed the usual procedure is to look for eigenfunctions and eigenvalues of:

$$\left(-\frac{d^2}{d\tau^2} + V''[\bar{x}(\tau_1)]\right)y_n(\tau) = \lambda_n y_n(\tau) \quad (2.24)$$

since it is of the Sturm-Liouville form, ie:

$$-\frac{d}{dx} \left[p(x) \frac{dy}{dx} \right] + q(x)y = \lambda w(x)y. \quad (2.25)$$

When properly normalised the y_n will form a total orthonormal Schauder basis for the Lebesgue space $L^2\left(\left[-\frac{T}{2}, \frac{T}{2}\right], 1dx\right)$ and hence we are able to express our fluctuations $\Delta x(\tau)$ in terms of an infinite sum of y_n :

$$\Delta x(\tau) = \sum_{n=0}^{\infty} \zeta_n y_n(\tau) \quad (2.26)$$

And so we can write

$$\begin{aligned} S_e^{fl} &= \frac{m}{2} \int \Delta x(\tau_1) \left(-\frac{d^2}{d\tau^2} + V''[\bar{x}(\tau_1)]\right) \Delta x(\tau_1) d\tau_1 \\ &= \frac{m}{2} \int \sum_{n=0}^{\infty} \zeta_n y_n(\tau) \sum_{m=0}^{\infty} \zeta_m y_m(\tau) \lambda_m d\tau_1 \\ &\quad \text{using the orthonormality of the } y_n \\ &= \frac{m}{2} \sum_{m=0}^{\infty} \zeta_m^2 \lambda_m. \end{aligned} \quad (2.27)$$

Now in order to sum over all variations of the path it is necessary to integrate over all values of the ζ_m . In making this transformation to the basis of y_n we have effectively transformed the integration of paths into a infinite product of real valued integrals. The ‘‘Jacobian’’ of such a transformation is not easily defined but it will not be necessary to determine the unknown constant N that is introduced:

$$\begin{aligned} \mathcal{F} &= \int \mathcal{D}[\Delta x(\tau)] e^{-\frac{S_e^{fl}[\Delta x(\tau)]}{\hbar}} \\ &= N \prod_{n=0}^{\infty} \int_{-\infty}^{\infty} \frac{d\zeta_n}{2\pi\hbar} \exp\left\{-\frac{m}{2\hbar} \zeta_n^2 \lambda_n\right\} \\ &= \frac{N}{\sqrt{\prod_{n=0}^{\infty} \lambda_n}} \end{aligned} \quad (2.28)$$

So the original path integral has now been reduced to

$$\langle x_f | e^{-\frac{\hat{H}\tau}{\hbar}} | x_i \rangle = e^{-\frac{S_e[\bar{x}(\tau)]}{\hbar}} \frac{N}{\sqrt{\prod_{n=0}^{\infty} \lambda_n}}. \quad (2.29)$$

2.4.3 Evaluating the infinite product

In order to evaluate the infinite product given in 2.29 it will be necessary to remove the normalisation N that was introduced when the path integral was transformed to a product of integrals over ζ_n . To do this consider the solution $x_0(\tau)$ where the position remains constant, this will be a stationary path with respect to the action, its fluctuation term \mathcal{F}_0 will have a fluctuation action of the form

$$\frac{m}{2} \int -\Delta x(\tau_1) \Delta x''(\tau_1) + \omega \Delta x(\tau_1)^2 d\tau_1 \quad (2.30)$$

with ω a constant. This is simply the fluctuation factor from a harmonic potential, which is exactly solvable. So we can write

$$\begin{aligned} \mathcal{F} &= \frac{N}{\sqrt{\prod_{n=0}^{\infty} \lambda_n}} = \frac{N}{\sqrt{\prod_{n=0}^{\infty} \lambda_n^0} \sqrt{\prod_{n=0}^{\infty} \lambda_n}} \quad (2.31) \\ &= \mathcal{F}_0 \frac{\sqrt{\prod_{n=0}^{\infty} \lambda_n^0}}{\sqrt{\prod_{n=0}^{\infty} \lambda_n}} \end{aligned}$$

There is still a possible divergence in the above expression that shall be addressed in the section below.

2.4.4 Zero Eigenvalue Solution

As the limits of the integration in the euclidean action tend to positive and negative infinity we expect that the contribution to the action from the soliton solution $x(\tau)$ to be translationly invariant. An instanton centered at τ_0 and another instanton, infinitesimally separated, centered at τ'_0 will give the same contribution to our euclidean action. The difference between these solutions manifests itself as a fluctuation around the instanton solution that does not change the euclidean action. As a consequence there will always exist an eigenfunction y_0 such that $\lambda_0 = 0$. As mentioned above the eigenfunction responsible for the divergence is $y_0 = \alpha x'(\tau - \tau_0)$. The key to removing this divergence is to evaluate the contribution resulting from the invariance of a single instanton, replacing the integral over ζ_0 with an integral over the position of the center of the instanton. Recalling that in order to form a basis the eigensolutions to equation (2.24) should be normalised we have $\alpha = \sqrt{S_\epsilon[\bar{x}(\tau)]}$. Our divergent contribution arises from the integral

$$\int_{-\infty}^{\infty} \frac{d\zeta_0}{\sqrt{2\pi\hbar}}. \quad (2.32)$$

Recalling that

$$x(t) = \bar{x}(\tau - \tau_0) + \Delta x(\tau) = \bar{x}(\tau - \tau_0) + \frac{m}{2} \sum_{m=0}^{\infty} \zeta_m^2 y_m \quad (2.33)$$

we have $\frac{dx}{d\zeta_0} = y_0$ and $\frac{dx}{d\tau_0} = \bar{x}(\tau - \tau_0)$ giving

$$\begin{aligned} x d\tau_0 &= y_0 d\zeta_0 \\ \Rightarrow d\zeta_0 &= \sqrt{S_e[\bar{x}(\tau)]} d\tau_0. \end{aligned} \quad (2.34)$$

So we make the replacement

$$\frac{1}{\sqrt{\lambda_0}} = \sqrt{\frac{S_e[\bar{x}(\tau)]}{2\pi\hbar}} \int_{-\frac{L}{2}}^{\frac{L}{2}} d\tau_0 \quad (2.35)$$

2.4.5 Key Results of the Double Well potential

Thus far our analysis has been a general motivation and definition, we now consider the specific results of the double well potential. Aspects of the derivation that are important to the analysis in further chapters are included in the appendix with the remaining technicalities left as references. The solution was calculated originally by Langer [13], however methods used in the appendix follow more closely the formulation given in the books by Kleinart [12] and Schulman [15]. We define the symmetric double well potential as the quartic function in equation (2.36) shown in figure (2.4.5)

$$V(x) = \frac{\omega^2}{8a^2}(x-2)^2(x+2)^2 \quad (2.36)$$

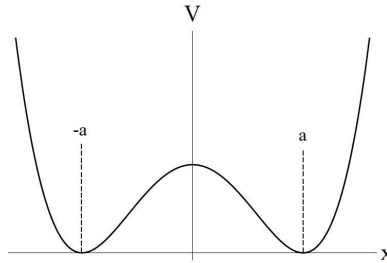


Figure 2.3: The Symmetric potential $V(x) = \frac{\omega^2}{8a^2}(x-2)^2(x+2)^2$

We are interested in the solutions to the Euler-Lagrange equations of the inverted potential in the zero temperature limit. In the limit $\tau \rightarrow \infty$ there exists an infinite number of solutions. We will need to evaluate explicitly only two, the first is the trivial solution where the particle starts and remains at $\pm a$, we shall refer to this as the trivial or degenerate solution. The second solution is

$$x(\tau) = \pm a \tanh\left(\frac{\omega}{2}(\tau - \tau_0)\right) \quad (2.37)$$

Which corresponds to the particle crossing to the other side minima. The $\tau - \tau_0$ reflects the fact that in the $\beta \rightarrow \infty$ limit the particle can spend infinite time at its

initial stationary point before crossing to the other stationary point where it remains indefinitely. While we will be interested in solutions valid for finite temperatures, we will see that the correction to this assumption are negligible.

Classical Contribution to the Action

We can now easily evaluate the “classical” contribution to the action. In the case of the constant solutions we have $S_e[x(\tau) = \pm a] = 0$. For the case of the non-trivial solution it is easily confirmed that

$$\int_{-\frac{\tau}{2}}^{\frac{\tau}{2}} d\tau \left(\frac{d}{d\tau} \pm a \tanh \frac{\omega}{2} (\tau - \tau_0) \right)^2 + V(\pm a \tanh \frac{\omega}{2} (\tau - \tau_0)) = \frac{2}{3} a^3 \omega \quad (2.38)$$

2.4.6 Fluctuation contribution to Feynman Kernel

We must now evaluate the contribution to the propagator equation (2.23) from the quadratic fluctuations around the action. We seek to diagonalize the fluctuation integral in order to reduce our problem to an infinite product of eigenvalues of the equation. We obtain (see appendix)

$$\left(-\frac{d^2}{d\tau^2} + \omega^2 \left(1 - \frac{3}{2 \cosh^2 \left(\omega \frac{(\tau - \tau_0)}{2} \right)} \right) \right) y_n(\tau) = \lambda_n y_n(\tau) \quad (2.39)$$

At this point we are left with the problem of evaluating the product of infinite eigenvalues, we have seen that one of these values approaches zero but that by considering the translation invariance of the instanton solution a finite contribution can be attributed. Conceptually we should now be able to reach our solution. There are, however, still two properties of the calculation that will cause us difficulty. The first is since we have argued that our instanton will decay exponentially to a constant far from the center of the instanton, for solutions of equation (2.39) with eigenvalues greater than the value of $\omega^2 \left(1 - \frac{3}{2 \cosh^2 \left(\omega \frac{(\tau - \tau_0)}{2} \right)} \right)$ we do not expect discrete values of the eigenvalues but rather a continuum of solutions. The second difficulty is that in addition to the instanton solution already obtained we expect that there should exist solutions that cross the barrier in the inverted potential multiple times. In the zero temperature limit there should in fact exist an infinite number of such solutions and we must account for the contributions from these solutions.

Eigenvalue Contribution and Multiple Instanton solutions

In the appendix it is shown that it is possible to write the ratio of products of eigenvalues as the ratio of solutions to two second order differential equations. We

then have the single instanton solution

$$\langle x_f | e^{-\frac{\hat{H}\tau}{\hbar}} | x_i \rangle = \sqrt{\frac{\omega}{\pi\hbar}} e^{-\frac{\omega L}{2\hbar}} \beta K e^{-\frac{S_e[x(\tau)]}{\hbar}} \quad (2.40)$$

where $K = \frac{\sqrt{\prod_{n=0}^{\infty} \lambda_n^0}}{\sqrt{\prod_{n=1}^{\infty} \lambda_n}}$ and we have let $x_f = a$ and $x_i = -a$. All that remains is to evaluate the contribution of the multiple crossing solutions. To do this we use what is referred to as the rare gas of kinks and anti-kinks [12]. Since the instanton is well localised and the range of the integration approaches infinity we approximate the remaining solutions as piece wise defined combinations of the single kink solution. To do this we use the symmetry of the potential, should we want a solution moving from x_f to x_i we could simply use negative of equation (2.36). For example consider a function that is equal to the instanton solution in one sub domain and a phase shifted negative solution in another we have a function that returns to x_i . An example of one such solution is shown in figure (2.4). This function should also be a solution to the Euler Lagrange equation with a small correction near transition between the sub domains.

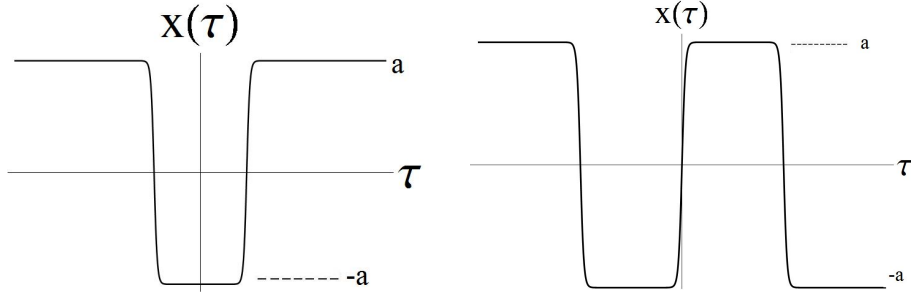


Figure 2.4: Left: A so called two kink or two instanton solution in which the system returns to the initial state. Right: A so called three instanton solution in which the system finishes in the opposite state. In the zero temperature limit we can continue to add kinks to create an infinite number of solutions

We could continue this procedure to create solutions that cross the barrier region numerous times as in figure 2.4. The resulting solutions are referred to as a rare gas of instantons. So called because of the particle like nature of our solution and the assumption that the instantons are sufficiently separated so that the contribution to our calculation from each one is essentially separate from the others. In the finite temperature approximation one expects that since the instantons have finite width and the range of our τ integration is finite that there must be an upper limit on the number of instantons that can be included in a solution before the assumption of spacing is violated. It is possible to show that the contribution from solutions with a high number of kinks N is suppressed by a factor of $\frac{1}{N!}$. Using this fact we sum

over all possible rare gas solutions to obtain

$$\langle \pm a | e^{-\frac{\hat{H}\tau}{\hbar}} | a \rangle = \sqrt{\frac{\omega}{\pi\hbar}} e^{-\frac{\omega\beta}{2\hbar}} \beta \times \frac{1}{2} \left[\exp\left(K\beta e^{-\frac{S_e[x(\tau)]}{\hbar}}\right) \pm \exp\left(-K\beta e^{-\frac{S_e[x(\tau)]}{\hbar}}\right) \right] \quad (2.41)$$

The two solutions have arisen because the solutions in the rare gas with an even number of crossing return to their initial locations, whereas the odd ones finish on the other side of the well. Comparison with the Feynman-Kac formula 2.15 would suggest that we have calculated the first two energy levels, even though we argued that higher energy level contribution should have been exponentially suppressed. The energies are

$$E_{\pm} = \hbar \left(\frac{\omega}{2} \pm K e^{-\frac{S_e[x(\tau)]}{\hbar}} \right) \quad (2.42)$$

Recalling that $S_e[x(\tau)] = \frac{2}{3}a^2\omega$ from equation (2.40) we see that the difference in the two energies is negligible and hence they both appear as the leading terms in semi-classical approximation. Note in limit of a tending to infinity we the potential will have the form of two uncoupled harmonic oscillators and the ground state energy will approach $\frac{\omega\hbar}{2}$ which is consistent with the known solution of the harmonic oscillator.

In this chapter we explained how the path integral formulation of quantum mechanics can be used to treat quantum tunneling problems through the Wick rotation. We also explained why the general techniques for evaluation. In the next section where we show for the first time that it is possible to treat the double well numerically. We then use this new method to treat make estimates of the value of competing solutions in a Multiferroic system.

Chapter 3

Numerical Treatment of Double Well Potential

In this section I present a new technique for making an approximation to the path integral. The technique is based on relaxation method commonly used in molecular dynamics. Unlike initial value differential equations where shooting methods are usually utilized, in order to approximate two point boundary value problems one starts with an initial paths that connects the boundary points. Then iteratively perturb the path towards the desired solution. Comparing this new technique with the known analytic solution should motivate the validity of the treatment prior to application to the more complex system considered in the fifth chapter. While the key results have been given in the first chapter the unfamiliar reader would benefit from following the analytic solution given in the appendix.

3.1 Finding the Stationary Path

The potential under consideration is the symmetric quadratic well,

$$V(x) = \frac{\omega^2}{8a^2}(x - a)^2(x + a)^2. \quad (3.1)$$

When we perform the imaginary time substitution as in section 2.2, the problem is now in the form of equation(2.9) with the euclidean action defined with $V(x)$ as above. From equation (2.19) we know that finding the stationary path will be equivalent to solving the Euler Lagrange equations for the inverted potential. We wish to solve $m\ddot{x} - V'(x) = 0$ where the dots represent the derivative with respect to the transformed time τ . In the zero temperature limit we have boundary conditions at $\tau = \pm\infty$, the system must return to one of the minima $x(\tau) \rightarrow \pm a$. In the numerical case we consider a total period of transformed time T and attempt to

find solution that crosses the barrier once. Our path will be represented by N discrete values evenly spaced in transformed time. T must be chosen sufficiently large, if the instanton width is of the same order as T we will not get an accurate approximation to the exponential decay rate away from the center of the solution. We define $\tau_i = \tau_0 + i\epsilon$ where $\epsilon = \frac{T}{N}$ and label the value of the function $x(\tau)$ at τ_i as x_i . In order to find the minimizing path we will use a chain of states method, to do so we will need to specify an objective function that will be minimised for our desired values of x_i . Since $m\ddot{x} - V'(x) = 0$ we consider

$$V_{\text{sup}}^i = (m\nabla\bar{\nabla}x_i - V'[x_i])^2 \quad (3.2)$$

where ∇ and $\bar{\nabla}$ represent the forward and backwards finite element approximation to the derivative respectively:

$$\nabla\bar{\nabla}x_i = \frac{x_{i+1} - 2x_i + x_{i-1}}{\epsilon^2} \quad (3.3)$$

taking the negative of the derivative of the above equation with respect to x_i gives a term for each x_i that gives the direction of maximum descent with respect to our objective function.

$$-\frac{d}{dx_i}V_{\text{sup}}^i = -2(\nabla\bar{\nabla}x_i - V'[x_i])\left(-\frac{2}{h^2} - V''[x_i]\right) \quad (3.4)$$

We then follow [8] and use equation(3.4) as the second derivative in the velocity verlet algorithm:

$$\begin{aligned} 1. \quad & \vec{x}(t + \Delta t) = \vec{x}(t) + \vec{v}(t) \Delta t + \frac{1}{2}\vec{a}(t)(\Delta t)^2 \\ 2. \quad & \vec{v}(t + \frac{\Delta t}{2}) = \vec{v}(t) + \frac{\vec{a}(t)\Delta t}{2} \\ 3. \quad & \vec{a}(t + \Delta t) = -\frac{1}{\text{constant}}\nabla V \\ 4. \quad & \vec{v}(t + \Delta t) = \vec{v}(t + \frac{\Delta t}{2}) + \frac{\vec{a}(t + \Delta t)\Delta t}{2} \end{aligned} \quad (3.5)$$

While the above approach gives reasonably rapid convergence in terms of the width of the solution, $O(10^3)$ iterations of the algorithm, the result that we obtain retains some numerical artifacts in the form of ‘humps’ (see figure (3.1)) where the solution first moves away from the central barrier before crossing over. To correct this the solution is used as the initial guess in a Monte-Carlo algorithm which also takes $O(10^3)$ iterations to converge to a smooth result. It is important to use the verlet algorithm first, if the Monte Carlo method were to run from a random guess it becomes necessary to use a far larger number of iterations.

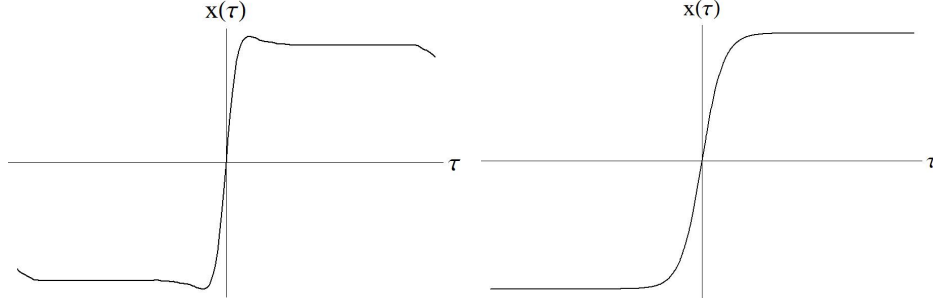


Figure 3.1: Left: The numerically determined path before Monte Carlo, showing the humps characteristic of this numerical treatment. Right: The numerically determined path after Monte Carlo, the 'hump' characteristic has been removed

3.1.1 Classical contribution

Once a path is determined we perform a simple integration to evaluate $S_e[x(\tau)]$. Below is a table of numerically and analytically obtained values. For each calculation the user defined values of T and N were kept constant at 8000 and 200 respectively. We see that it is possible to obtain values from a variety of potential parameters with a single choice of T and N , indicating the robustness of the algorithm.

Minimum Spacing	$V_{\max} = \frac{(aw)^2}{8}$	Numerical Value	Analytic Value
1	2.812510^{-7}	0.000502217	0.0005
2	0.0000125	0.00665781	0.00666667
4	0.00125	0.13852	0.133333

3.2 Discrete Eigenvalue Contribution

Now that the classical path has been determined we can make an approximation to the integral using equation A.8 from page 45 of the appendix.

$$\langle -a | e^{-\frac{\hat{H}\tau}{\hbar}} | a \rangle \approx e^{S_e[\bar{x}(\tau)]} \int \mathcal{D}[\Delta x(\tau)] e^{-\frac{S_e^{fl}[\Delta x(\tau)]}{\hbar}} \quad (3.6)$$

with

$$S_e^{fl} = -\frac{m}{2} \int -\Delta x(\tau_1) \Delta x''(\tau_1) + \frac{d^2}{dx^2} V(\bar{x}(\tau_1)) \Delta x(\tau_1)^2 d\tau_1 \quad (3.7)$$

We now have to sum over fluctuations around the stationary path. We will represent the fluctuation away from the classical path by $\Delta x(\tau)$. In order to evaluate the path integral as a product of Gaussian integrals we will need to find an approximation to the eigenvalues of the differential equation A.28. We approximate this basis for the fluctuations by

$$(-\nabla \bar{\nabla} + \underline{\underline{V}}) \mathbf{y}_n = \lambda_n \mathbf{y}_n \quad (3.8)$$

Where the \mathbf{y}_n are N vectors representing the fluctuations, $-\nabla\bar{\nabla}$ represent a tri-diagonal matrix

$$-\nabla\bar{\nabla} = \frac{1}{\epsilon^2} \begin{pmatrix} -2 & 1 & & & & \\ 1 & -2 & 1 & & & \\ & 1 & -2 & 1 & & \\ & & & \dots & & \\ & & & & \dots & \\ & & & & & \dots \end{pmatrix}$$

and

$$\underline{V}_{ij} = \delta_{ij}V[x_i]. \quad (3.10)$$

We proceed by finding the eigenvalues of this matrix. The smallest eigenvalues will correspond to the discrete eigensolutions. Note that the equation we are solving has the same form as a Schrödinger equation and that the potential will be well localised (since it has explicit dependence on the stationary solution, which was well localised) negative and approaching a constant exponentially. Due to the well localised nature of the potential we expect only a finite number of bound state like solutions to this equation and then a continuum of unbound solutions. In order to determine how many discrete solutions exist and correspondingly how many eigenvalues we should take from this matrix it is necessary to view the eigenvectors of equation(3.8). Eigenvectors corresponding to continuum eigenvalues (those we wish to disregard) will take the form of sinusoidal solutions with a phase shift at the potential. Since in our discrete approximation τ will be defined only over a finite interval hence the solutions will have finite support (in the approximation these solutions will be analogous to a particle in a box with a small perturbation at the origin. Those solutions corresponding to the bound state type solutions should be well localised. In figure (3.2) the first four eigenfunctions of the matrix plotted against τ

Using the stationary paths obtained in the previous section we can calculate the discrete eigenvalues and again compare with the known analytic results.

minima spacing	Vmax	First Eigenvalue	Second Eigenvalue	Analytic Second
2	0.0000125	-1.81942×10^{-8}	0.0000746241	0.000075
1	2.812510^{-7}	-2.95857×10^{-7}	6.14927×10^{-6}	6.75×10^{-6}
4	0.00125	-0.000443809	0.00121277	0.001875

3.3 Continuum Eigenvalue Contribution

Having determined the classical path, its contribution and the discrete eigenvalues in the expansion all that remains is the determination of the product of continuum

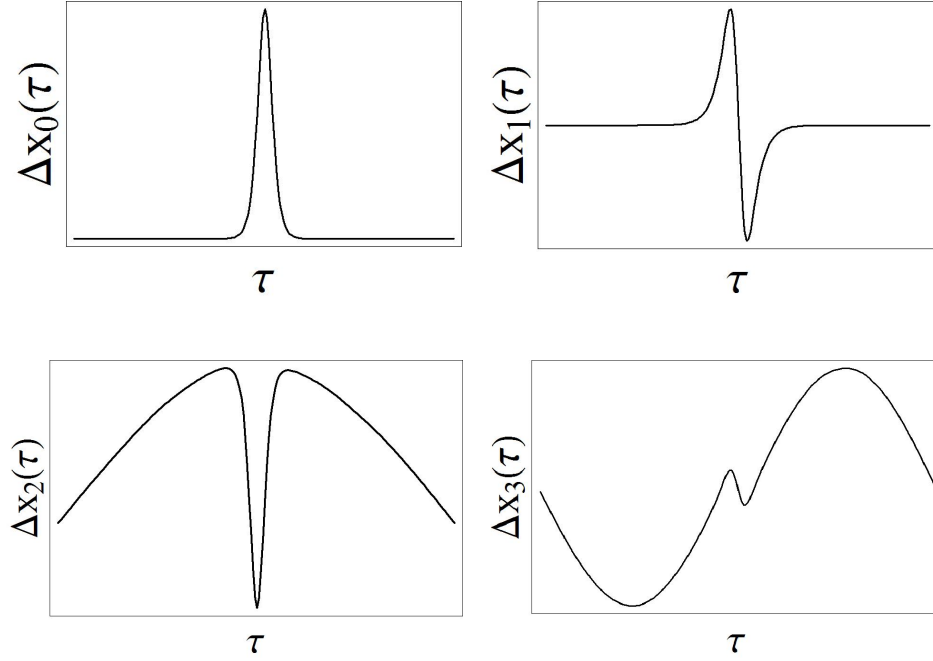


Figure 3.2: In the above we see the first four eigen solutions. Top right: the single kink solution corresponding to the zero eigen value mode. Top left: the first positive eigen value mode this is the only discrete eigen value. Bottom: The third and fourth eigen value modes, these are members of the continuum of eigen value solutions

eigenvalue solutions. From [15] we know that the product can be written in terms of the ratio of solutions to two differential equations.

$$\frac{1}{2} \frac{d^2 f(\tau)}{d\tau^2} = -\frac{1}{2} V''[\bar{x}(\tau)] \frac{f(\tau)}{m} \quad (3.11)$$

and

$$\frac{d^2 f^0(\tau)}{d\tau^2} = -\omega^2 \frac{f^0(\tau)}{m} \quad (3.12)$$

where ω^2 was obtained by considering the contribution from the degenerate instanton solution. In the appendix we show that we are interested in evaluating the object

$$R^2 = \frac{f^0(\beta) \lambda_1 \lambda_0}{f(\beta)} \quad (3.13)$$

Both with the boundary condition

$$\begin{aligned} f(0) &= 0 \\ \frac{df(0)}{d\tau} &= 1. \end{aligned} \quad (3.14)$$

Since β will be large in the small temperature limit then we can easily approximate the differential equation related to the degenerate solution with (as in the appendix):

$$f^0(\beta) \approx \frac{1}{2\omega} e^{\beta\omega} \quad (3.15)$$

where ω is found by approximating the minima by a quadratic equation. this leaves only the first equation, as in the appendix the solution to this problem can be obtained from the instanton. The derivative of the stationary solution (the eigenfunction corresponding to the zero eigenvalue solution) will satisfy equation 3.11) but will fail to satisfy the boundary conditions. There must, however, exist a second linearly independent solution such that the two can be combined to satisfy the boundary conditions.

$$f(\tau) = c_1 f_1(\tau) + c_2 f_2(\tau) \quad (3.16)$$

Since we are interested in evaluating the functions for large τ we only need to account for asymptotic behavior. In this limit the zero eigenvalue solution will take the form of a decaying exponential. We can therefore approximate the exponential by matching it the decaying edge of the numerically determined zero solution. This does however have the potential to cause some difficulty; close to the center of the numerical solution the approximation to an exponential is not valid, however, the actual solution is expected to approach zero at $\pm\infty$ while our numerical solution reaches zero in a finite time. Provided we make the imaginary time interval in which we approximate the zero eigenvalue solution sufficiently large there should be a region between the center and the end points where the approximation to an exponential is sufficiently good. Having now approximated the asymptotic behavior of one solution we can easily approximate the other. In order that the second solution be linearly independent we require that the wronskian of the two solutions be non zero, since we have already argued that the form of the solutions should be exponential we let the Wronskian be equal to one

$$f_1 f_2' - f_2 f_1' = 1 \quad (3.17)$$

Combining this with the boundary conditions we obtain $c_1 = -f_2(0)$ and $c_2 = f_1(0)$ from which we can show that $f(\beta) = \frac{1}{\kappa}$. The remaining two discrete eigenvalues are all that remain to be evaluated. The nonzero eigenvalue will already have been determined leaving us with the zero eigenvalue to approximate, fortunately when the temperature is non-zero it is possible to show that [15]

$$\lambda_0 \approx \frac{f_1(\beta)}{f_2(\beta)} \quad (3.18)$$

And hence we have all the information we need to make an approximation to the path integral

3.3.1 Level Splitting formula

Following the argument in the appendix we can combine our calculated values to obtain values for the level splitting formula. As in the appendix we define K for

convenience

$$K = \sqrt{\frac{S_e[\bar{x}(\tau)]}{2\pi}} \frac{1}{\sqrt{|\lambda_{-1}|}} \sqrt{\frac{\prod_n^0 \lambda_n}{\prod_{n \neq 0,1} \lambda_n}}, \quad (3.19)$$

And recall that the magnitude of the level splitting was

$$\Delta E = 2K\hbar e^{-\frac{S_e[\bar{x}(\tau)]}{\hbar}}. \quad (3.20)$$

In tables (3.1) and (3.2) we see that our approximation agrees strongly with the analytic values for the first two entries. In the third entry we used a tall potential leading to wide instanton solution, but we did not change the parameter T in the numerical algorithm. Our third solution is therefore close to the limit of potential we can treat with a single choice of parameter. We observe that there is a large range of barrier heights that can be treated with a single choice of T making the algorithm fairly robust.

Table 3.1: Table comparing the values of the exponent $-\frac{S_e[\bar{x}(\tau)]}{\hbar}$

$V_{\max} = \frac{(aw)^2}{8}$	Numerical exponent (10^{30})	Analytic exponent
2.812510^{-7}	-4.76229	-4.74126
0.0000125	-63.1328	-63.2168
0.00125	-1385.2	-1264.3

Table 3.2: Table comparing the values of the prefactor $2K\hbar$

$V_{\max} = \frac{(aw)^2}{8}$	Numerical Prefactor (10^{-21})	Analytic Prefactor
2.812510^{-7}	1.96258	1.90404
0.0000125	22.5695	23.1752
0.00125	244.926	518.213

Chapter 4

Metastable States

In this chapter we explain how the preceding calculations differ when treating a potential that is not symmetric an example is shown in figure 2.2 in section 2.2. In order to formulate a metastable formalism we will use the results formulated in the second chapter and discuss how the results differ for asymmetric potentials. We continue to use the path integral formalism of the preceding chapters. Recall that transformed propagator had the form of a partition function, we will calculate the propagator despite starting in a state that we expect to decay. We have stipulated that the life time of the state be large compared to the time scale of any other processes occurring. We will show that for the metastable state there exists a destabilizing fluctuation that manifests itself as an imaginary part to the free energy. We will associate this imaginary part with the rate of decay of the metastable state.

Consider figure 2.2, where the system is in a local minimum separated from a lower minimum by a barrier. Using the Feynman-Kac formula (2.15) on page 10 we could proceed as with the double well problem to calculate the ground state energy. By comparison with the double well potential we would arrive at the equation 4.1. Unlike the symmetric case, when we consider the inverted potential there is no solution corresponding to a single crossing of the barrier. Instead the simplest non degenerate solution corresponds to a particle leaving the metastable minimum moving towards the other minimum, at some “time” before reaching the minimum the particle will have reached a point of where the potential has the same value as the metastable minimum, see figure (4.1). The particle will then return to the metastable state. And so we will not have considered ‘odd’ and ‘even’ solutions as before. The imaginary time propagator will now have the form

$$G(x, \frac{L}{2}; x, \frac{L}{2}) = F_\omega \exp \left[\left(\frac{S_e[\bar{x}(\tau)]}{2\pi\hbar} \right)^{\frac{1}{2}} K' \beta e^{\frac{S_e[\bar{x}(\tau)]}{\hbar}} \right] \quad (4.1)$$

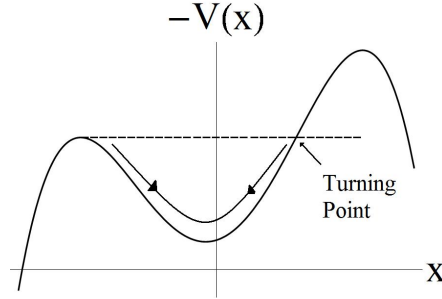


Figure 4.1: In the inverted potential simplest solution will cross the barrier region and return to the location of the metastable minimum

where x is location of the local minimum, β is the large τ limit of our integration and K' is the ratio of eigenvalues excluding the zero eigenvalue.

$$K' = \sqrt{\frac{\prod_n^0 \lambda_n}{\prod_{n \neq 0} \lambda_n}} \quad (4.2)$$

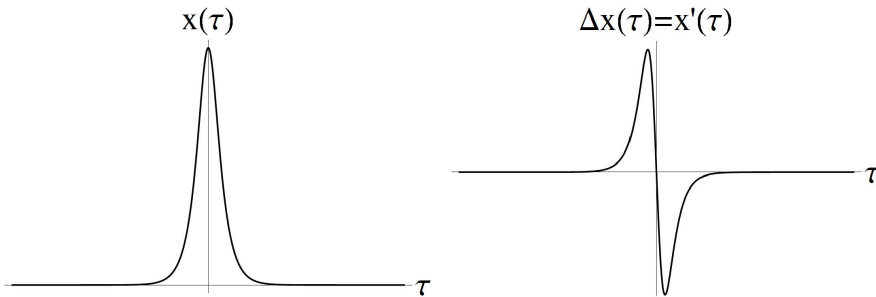


Figure 4.2: Left: The instaton must have a turning point. Right: The derivative of the instaton which will satisfy the Euler Lagrange equations in the inverted potential

We argued that for the metastable case there was only the single class of solution where the instaton solution will start and finish in at the local minimum, then the solution must have a turning point as in figure (4.2). Now from the appendix and equations A.8 A.9 we know that when we diagonalize the fluctuation contribution to the propagator that we will be looking for solutions to the equation

$$\left(-\frac{d^2}{d\tau^2} + V''[\bar{x}(\tau)]\right)y_n(\tau) = \lambda_n y_n(\tau) \quad (4.3)$$

and that there will exist a solution proportional to the derivative of $\bar{x}(\tau)$ that will create a zero even value λ_0 . The derivative of a single node solution should have two nodes. However $V''[\bar{x}(\tau)]$ will exponentially decay towards a constant away from t_0 and thus take the form of a well localised potential. There must exist a one node

solution. This one node solution should have an eigenvalue smaller than the two node solution, a negative eigenvalue λ_{-1} . The propagator will now carry an integral contribution of the form

$$\int \frac{d\zeta}{\sqrt{2\pi\hbar}} e^{\frac{\zeta^2 \lambda_{-1}}{2\hbar}} \quad (4.4)$$

If we allow ζ to be imaginary a careful analytic continuation can be performed the details of which are given in [12]. The result is

$$\int \frac{d\zeta}{\sqrt{2\pi\hbar}} e^{\frac{\zeta^2 \lambda_{-1}}{2\hbar}} = \frac{i}{2\sqrt{|\lambda_{-1}|}}. \quad (4.5)$$

Mathematically this analytic continuation is somewhat involved and the factor of a half is unexpected (consider evaluating for λ_0 positive and then make a substitution of a negative value). However, we will see in the next section that it has an important physical interpretation.

4.1 Semi-Classical Tunnelling Formula

Now that the negative eigenvalue is to be included when we compare equations (4.1) to (2.15) on pages prop FKF and observe that the ground state energy will have an imaginary part

$$E_0^{\text{im}} = \left(\frac{S_e[\bar{x}(\tau)]}{2\pi\hbar} \right)^{\frac{1}{2}} K' e^{\frac{S_e[\bar{x}(\tau)]}{\hbar}} \quad (4.6)$$

with

$$K' = \sqrt{\frac{\prod_n^0 \lambda_n}{\lambda_{-1} \prod_{n \neq 0} \lambda_n}} \quad (4.7)$$

It is important to now understand the origin of this imaginary part of the energy as well as its interpretation. In the formulation of equation (2.15) it was necessary to approximate the contribution to the propagator in the low temperature limit by only the contribution from the lowest energy even value, we assumed the existence of a complete set of energy eigenfunctions. Our assumption is that the particle is most likely to be found in the minimum energy state of this basis. Such a state is clearly non existent; consider the limit of $T \rightarrow 0$ in this case (the absence of thermal fluctuations. It would be possible to prepare a particle into this state indefinitely. We know from other treatments of barrier systems that tunneling occurs. This is integral to our interpretation of E_0^{im} . Recall the time evolution of a quantum state of energy E_0 is given by

$$\begin{aligned} \Psi(x, t) &= \varphi(x) e^{\frac{-iE_0 t}{\hbar}} \\ &= \varphi(x) e^{\frac{-iE_0^{\text{re}} t}{\hbar}} e^{\frac{-\Gamma t}{2\hbar}}, \end{aligned} \quad (4.8)$$

where we have let $E_0^{\text{im}} = \frac{-\Gamma}{2}$ recalling that we have argued that E_0^{im} is negative so Γ is positive and the norm of this state evolves according to

$$\int d^3x \varphi(x)^* \varphi(x) = e^{\frac{-\Gamma t}{\hbar}} \quad (4.9)$$

And so using equations (4.9) and (4.6) we have arrived at the semi-classical tunnelling formula

$$\frac{\Gamma}{\hbar} = \left(\frac{S_e[\bar{x}(\tau)]}{2\pi\hbar} \right)^{\frac{1}{2}} |K'| e^{\frac{-S_e[\bar{x}(\tau)]}{\hbar}} \quad (4.10)$$

In the above equation the pre-factor is usually denoted the “bubble decay frequency” or “attempt frequency” and the exponential is referred to as the “quantum Boltzman factor”. If we consider the formulation only to zeroth order, ignoring the fluctuation terms, the life time of the metastable state would be indefinite. It is only with the inclusion of the fluctuation term that the metastability manifests itself in the formulation. The instability of the state is contained in the analytically continued negative eigenvalue term. We consider the factor of a half as describing the fact that the instability will only have a fifty percent chance to cause the system to move into equilibrium (it is equally likely that the system will be destabilized back into the metastable state).

Chapter 5

Application to Multiferroic System

In this chapter we describe a multiferroic system with coupled domain walls with the aim of deriving the Euler Lagrange equations for this system with an inverted potential. The solution to this equation will specify the instaton. We are then able to consider various behaviors of the system by analysing it with the numerical approximation described in chapter 3. In the following we treat the domain wall propagation with a one dimensional approximation, we do not account for effects due the curvature of the walls. In this treatment it is assumed also that the domain wall and the defect are a sufficiently separated from other defects or the surface of the material so that it is possible to integrate the energy densities between positive and negative infinity.

5.1 Representation of The Domain walls

5.1.1 Magnetic Domain Walls

To describe the magnetic domain wall, we will consider the profile that minimises the competing exchange energy and an anisotropy energy along the z axis. The exchange energy is a purely quantum mechanical effect which is a manifestation of the Coulomb interaction and Pauli exclusion principle [2]. Since the exchange energy favours uniform magnetization, the minimum energy configuration will favour large wall widths.

$$E_{\text{ex}} = \frac{JS^2}{a} \int_{-\infty}^{\infty} dz \frac{\partial \phi(z)^2}{\partial z}, \quad (5.1)$$

where J is the exchange integral (see [2]), S is the spin, a the crystal lattice spacing and ϕ is the angle that the magnetization makes with the z axis.

The anisotropy energy arises due to the structure of the crystal lattice that exist in a solid. Due to crystal symmetries in the absence of a magnetic field, ferromagnetic materials will be magnetized along certain energy favoured directions, known as “easy” directions or the easy axis of a material. If the z axis is perpendicular to the easy axis we have an energy density of the form.

$$E_a = \int_{-\infty}^{\infty} dz g(\phi) \quad (5.2)$$

$$\text{where} \quad g(\phi) = K \cos^2(\phi),$$

where ϕ is the angle between z and this axis and K is the anisotropy strength. It is easy to show that the magnetization profile that minimizes the functional $E_{\text{total}}[\phi(z)] = E_{\text{ex}}[\phi(z)] + E_a[\phi(z)]$ is

$$\phi(z) = \arctan(e^{(z)(\frac{K}{A})^{\frac{1}{2}}}) - \frac{\pi}{2}. \quad (5.3)$$

In obtaining this solution we have assumed that the magnetization is of constant magnitude and constrained in the $y - z$ plane at an angle ϕ to the z axis. We have described a wall where the magnetisation is rotated perpendicular to the wall surface, this is known as a Néel wall. The above solution will act as a prototype domain wall and describe an arbitrary domain wall profile with the two parameter function.

$$\varphi(z_M, \delta_M; z) = \arctan(e^{(z-z_M)\frac{\pi}{\delta_M}}) - \frac{\pi}{2}, \quad (5.4)$$

where the z_M is the location of the center of the magnetic domain wall and δ_M is the width.

5.1.2 Polarization Domain Walls

We continue in a completely analogous way to find a prototype profile for the polarization. The polarization must minimize the Landau Ginzberg energy density which is derived from symmetry arguments, see [14]

$$E[P(z)] = \int_{-\infty}^{\infty} dz \left(\alpha P^2 + \beta P^4 + \gamma \left| \frac{dP}{dz} \right|^2 \right) \quad (5.5)$$

where α , β and γ are phenomenological constants. One can easily show that the solution minimising the above functional is

$$P(z) = \sqrt{\frac{\alpha}{2\beta}} \tanh\left(\frac{\alpha}{2\beta\gamma} z\right). \quad (5.6)$$

As for the magnetic domain wall we define the domain wall in terms of the two parameter function

$$P(z_p, \delta_p; z) = \sqrt{\frac{\alpha}{2\beta}} \tanh\left(\frac{2}{\delta_p}(z - z_p)\right) \quad (5.7)$$

5.1.3 Width Dependence of Energy

We can now calculate the effect on the total energy of varying the domain wall position and width. Substituting our domain wall expressions (5.7) and (5.4) into the above energies (5.12)(5.13)(5.15). We obtain the following energy dependence

$$E(\delta_p, \delta_m) = \frac{2\pi A}{\delta_m} + \frac{2K\delta_m}{\pi} + \frac{4}{3} \frac{\gamma\alpha}{\beta\delta_p} + \frac{\alpha\delta_p}{3\beta} \quad (5.8)$$

5.2 Driving Force, Defect and Coupling

We must now define the remaining energy terms in the potential; the energy near the defect, the energy due to the domain wall coupling and the energy from the field. We will consider a barrier to the domain wall propagation, represented by a planar defect in the material. A suitable expression for the energy profile of a planar defect is given in [9] where a fractional change in the anisotropy (K) energy leads to a pinning energy of the form

$$E_{\text{defect}} = \rho K \sqrt{\frac{A}{K}} \text{sech}^2 \left(z_m - z_P \sqrt{\frac{K}{A}} \right) \quad (5.9)$$

where ρ is the strength of the defect.

The the coupling between the magnetization and the polarization will be described by an energy density of the form $E_{\text{coupling}} = c_s M^2 P^2$, where M denotes the magnitude of the magnetisation parallel to the polarisation and c_s is a constant. Hence substituting in our functions 5.4 5.7 with $M = M_0 \sin(\phi)$ and letting $D = z_m - z_P$ be the distance between wall centers we can write

$$E_{\text{coupling}} = c_s M \sqrt{\frac{\alpha}{2\beta}} \int_{-\infty}^{\infty} dz \left(1 - \tanh^2 \left(\frac{2}{\delta_p} (z - D) \right) \tanh^2 \left(\frac{\pi}{\delta_m} (z) \right) \right). \quad (5.10)$$

in obtaining the above expression we have made a change of variable to shift the $D = z_M - Z_E$ into one of the tanh. Writing the expression like this emphasizes the translational invariance of the coupling energy (the fact that it is only the distance between the walls that is of importance). Equation (5.10) is plotted in figure (??) In which we see two essential features; first that this term in the potential is symmetric and it rapidly approaches a constant. Considering the negative of the derivative of this energy with respect to z_m or Z_P we see that the force on the domain walls is attractive with limited range. Despite the attractive potential between them, if sufficiently far apart the force becomes negligible and walls are essentially decoupled. Finally the term driving the movement of the electric domain wall, an external

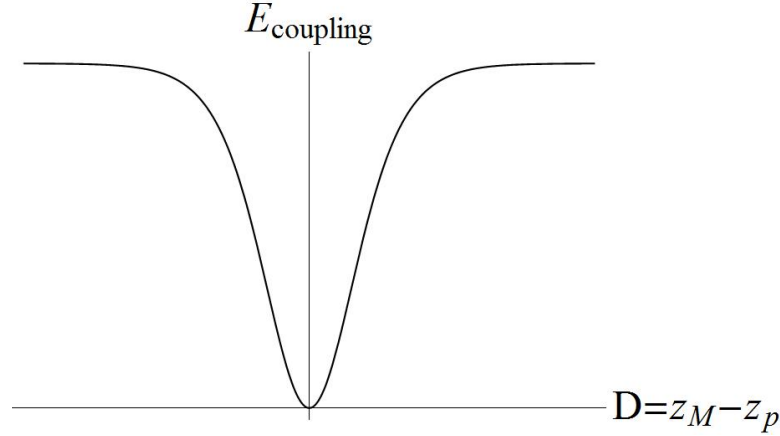


Figure 5.1: The two important aspect of the coupling energy are that it is symmetric and that it approaches a constant far from $D = 0$, where the electric and magnetic domain walls collide

electric field. It is easy to show that for the non deforming wall we have (add from notes)

$$E_{\text{driving}} = 2\sqrt{\frac{\alpha}{2\beta}}\mathcal{E}z_p \quad (5.11)$$

Where \mathcal{E} is the applied electric field and z_P is the position of the electric domain wall.

5.3 Domain Wall Inertia

Having obtained static energy terms to be used in the analysis, we now need to consider the inertia of the domain wall in order to associate a kinetic energy associated with domain wall movement. In our treatment we will assume that the system has evolved under the influence of the electric field an that it has reached the metastable minimum. We will assume also that the wall profiles remain static during the tunnelling. The change of the inertia of the domain walls due changes in the width is small and we do not expect that it should greatly effect our solution. It is necessary to associate an inertia with the position of the domain walls. The effective mass per unit area of the magnetic wall is given by [1] [16]

$$m_M = \frac{\sigma}{v_0^2}, \quad (5.12)$$

Where σ is the energy per unit area of wall and v_0 is the so called Walker velocity $v_0 = 4\pi\gamma_1 M_0 \sqrt{\frac{JS^2}{aK}}$. For the case of the effective mass per unit area of the polarisation domain wall we have[10]

$$m_E = \frac{Md^2}{Na^4} \quad (5.13)$$

where M is the mass of the ions that have been displaced leading to the polarization and d is the difference in displacement between two domains. N is the width of wall in terms of number of lattice constants a

5.3.1 Euler Lagrange Equations

Combining the above energies (5.12)(5.13)(5.15) and our expressions for the inertia of the domain walls the condition that $\delta S_e[\vec{z}] = 0$ for $\vec{z} = (z_m, z_P)$ after the Wick rotation gives us the following Euler Lagrange equations.

$$m_M \frac{d^2 z_M}{d\tau^2} + 2K \operatorname{sech} \left(\frac{z_M}{AK} \right)^2 \tanh \left(\frac{z_M}{AK} \right) - \int_{-\infty}^{\infty} dz 4 \frac{1}{\delta_E} \operatorname{sech}^2 \left(\frac{2(z-D)}{\delta_E} \right) \tanh \left(\frac{2(z-D)}{\delta_E} \right) \tanh \left(\frac{2(z-D)}{\delta_M} \right) = 0 \quad (5.14)$$

and

$$m_P \frac{d^2 z_P}{d\tau^2} - 2\sqrt{\frac{\alpha}{2\beta}} \mathcal{E} + \int_{-\infty}^{\infty} dz 4 \frac{1}{\delta_E} \operatorname{sech}^2 \left(\frac{2(z-D)}{\delta_E} \right) \tanh \left(\frac{2(z-D)}{\delta_E} \right) \tanh \left(\frac{2(z-D)}{\delta_M} \right) = 0$$

We can find an approximate solution to these equations using the numerical technique described in chapter 2 and hence obtain our instanton. In the next section we discuss general features of the potential and results from performing a numerical evaluation completely analogous to numerical evaluation of chapter 2.

5.4 Determining the End Points: Multiple Solutions

In order to make an approximation of the instanton solution it is necessary to calculate the location of the initial position and turning point of the instanton. Unlike the case of the simple one dimensional potential, the location of the metastable minimum is not likely to be determined analytically. However a simple numerical approximation is easily made. In the coupled domain wall system we have the advantage that in the absence of the coupling term the minimum configuration could be easily established. This configuration serves as a good initial choice of parameters for our minimization. Once this initial point is determined one must calculate the approximate location of the point where the potential will be equal to the metastable minimum, this is the location of the turning point of the instanton essentially defining the width of the barrier. Unfortunately unlike the one dimensional case we now have the problem that the equation $V(\vec{z}) = \text{Constant}$ now defines a multi-dimensional surface as we can see in figure 5.4. We will approximate the contribution to the tunnelling by taking the

point that is locally the point of closest approach to the minimum to be the location of the other side of the well. While this point will not be fixed during the subsequent evaluation of the instanton solution, a poor approximation will dramatically increase to the computation time required. We use the method of Lagrange multipliers to define an objective scalar function. we wish to minimise the potential width $W(z_m, z_P) = \sqrt{(z_P - z_{P0})^2 + (z_m - z_{m0})^2}$ subject to the constraint $V(z_m, z_P) - V_{\text{metastable}} = 0$. If we consider the $G(z_m, z_P, M) = W(z_m, z_P) - M(V(z_m, z_P) - V_{\text{metastable}})$ then we require $\nabla_{z_m, z_P, M} G(z_m, z_P, M) = 0$ which will be equivalent to minimising the scalar function

$$(\nabla_{z_m, z_P, M} G(z_m, z_P, M)) \cdot (\nabla_{z_m, z_P, M} G(z_m, z_P, M)) = 0, \quad (5.15)$$

which we minimize using basic monte Carlo.

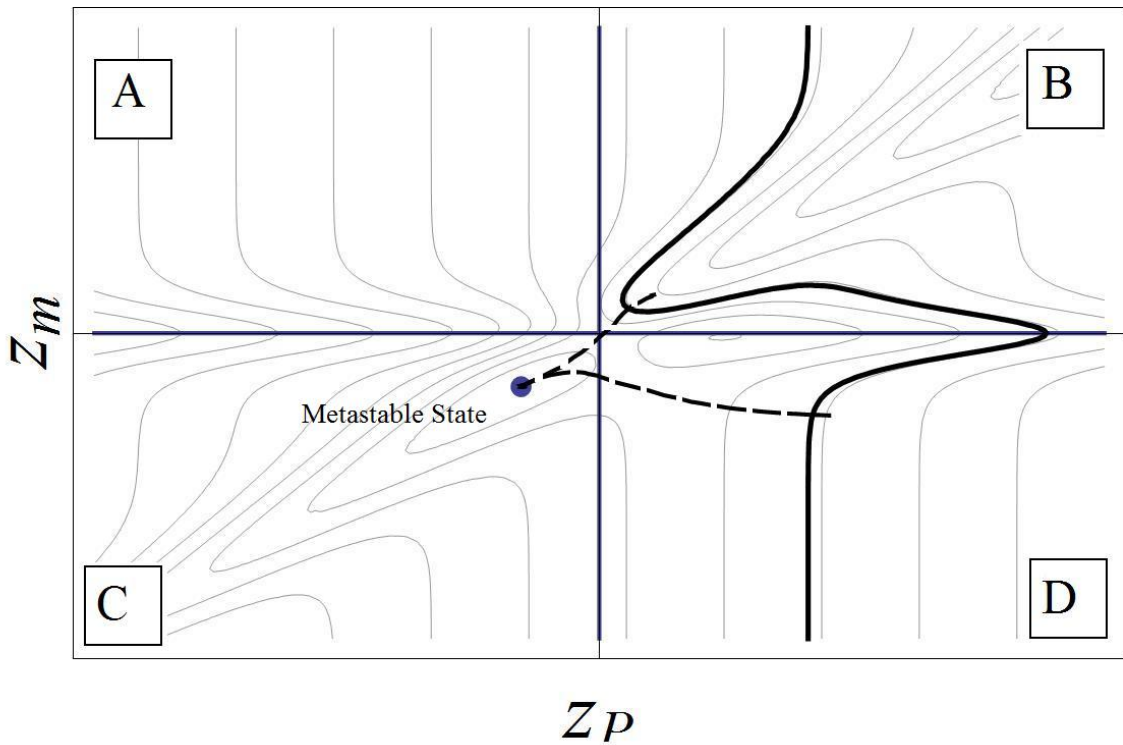


Figure 5.2: The potential energy space, in which one can see the two possible locally minimal distances from the metastable minimum to the equipotential surface. The instantons are shown by dashed lines.

In figure (5.4) we see a plot of the potential energy space along with the equipotential surface equal to the potential at the metastable minimum. The bold vertical and horizontal lines represent the center of the defect. We see the point marked corresponding to the location of the metastable minimum in the third quadrant. In the first quadrant one can observe a point that is locally the point of closest approach to metastable minimum, corresponding to the solution in which both the

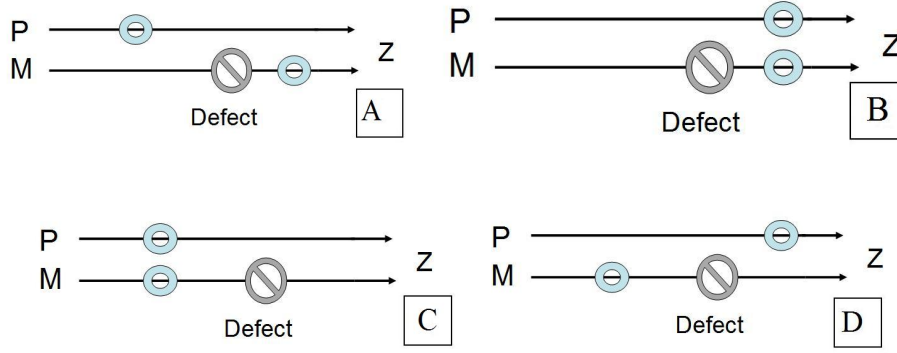


Figure 5.3: the various possible positions of the domain walls note that the equipotential line in figure (5.4) does not cross into region A indicating that the magnetic wall cannot tunnel independently of the domain wall

electric and magnetic domain walls are able to tunnel to the other side of the defect. We observe that the equipotential surface does not appear in the second quadrant. This should not be surprising at all, we do not expect a solution where the magnetic wall tunnels through the barrier and the electric wall remains behind. Since we are driving the only the electric wall this clearly would correspond to a configuration of the system that is physically forbidden. Finally in the fourth quadrant we see that there is another point on the equipotential that is locally a point of closest approach. This corresponds to the solution in which the magnetic wall remains pinned and the electric wall is able to tunnel through the barrier created by the coupling term and effectively decouple from the magnetic domain wall. In the following we will calculate the life times associated with both of these solutions and compare in order to see which is the dominant behavior.

5.5 Varying the applied field

We consider an arbitrary set of parameters and vary the electric field that is driving coupled domain walls towards the barrier. Observing the log plot below we see that varying the electric field does not change the final state of the system. In the plot (5.4) the coupled is has a far higher tunneling rate than the uncoupled solution.

Physically we can understand this lack of dependence by realizing that the applied electric field driving the system into equilibrium does not favor either solution. It appears then that the relative size of the coupling energy and the magnetic barrier should dominate our solution.

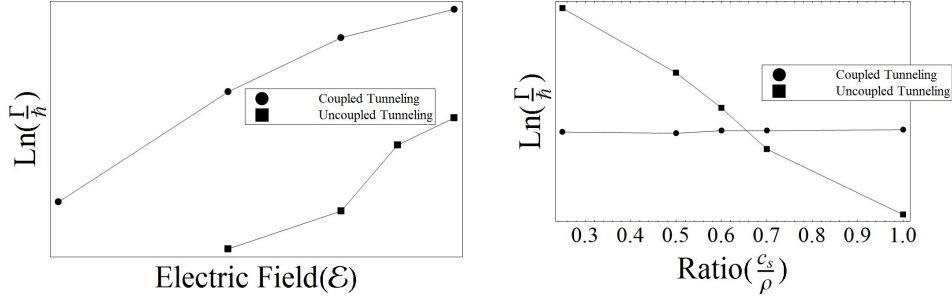


Figure 5.4: Left: The relative tunnelling rates of the two solutions; we see changing the electric field does not change the dominant solution. Right: In the above figure we see the relative coupling rates of the possible solutions, coupled tunneling (circles) and decoupling (squares) as a function of coupling strength do defect strength ratio.

5.6 Varying the coupling strength

We again choose an arbitrary set of parameters but this time consider the effect of varying the ratio of coupling strength (c_s) and the defect strength (ρ). The results are shown in figure (5.4). In the limit of no coupling the polarisation domain wall will experience no barrier while the magnetic domain experiences no driving force. In the absence of the coupling term we will no longer be treating a metastable tunneling problem. We do however expect that when the coupling is sufficiently weak that the decoupling solution should become dominant. In the limit of strong coupling we expect that both walls should tunnel. In the log plot showing the tunneling rates of the two possible solutions (5.4) we see that the tunnelling rate when the domain walls remained coupled is not effected greatly by the coupling strength, while the uncoupled solution is dramatically favored by a weak coupling.

We can gain understanding into this behavior by considering the form of the instaton solutions. In figure 5.4 we see that in order to tunnel into a lower energy state the walls must cross one of two saddle points. Consider a typical instaton solution shown in figure 5.5

in which the straight lines represent equipotential lines of the coupling energy with the dashed line representing zero energy (zero distance between the walls). We see that the for the coupled instaton solution the instaton remains close to the zero coupling energy. The height of the saddle point representing the tunneling barrier is dependent only on the defect, in this solution the walls act as a single object. Conversely if we consider the case decoupling, we see in figure 5.5 that the instaton has to cross the coupling equipotential lines. Changes to the coupling strength should greatly effect the tunneling rate of this solution. This solution only becomes

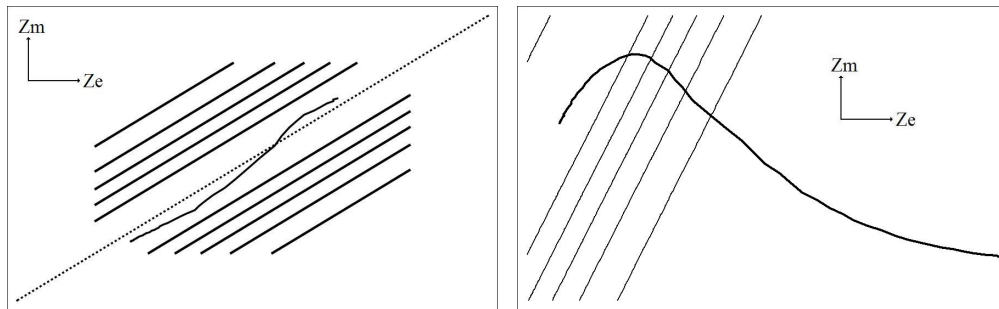


Figure 5.5: Left: Here we the instaton corresponding to the solution of coupled tunneling. The instaton closely follows the dashed line representing zero distance between the domain walls. Right: Here we the instaton corresponding to the solution of decoupling. Notice the instaton has to cross the coupling equipotential lines.

available if the coupling strength is sufficiently small.

Chapter 6

Conclusion

In this thesis we have investigated numerically the macroscopic tunnelling rates of a multiferroic system with coupling between electric and magnetic domain walls.

We began by explaining the formalism for treating quantum tunneling problems using a functional integral. In this formalism it is possible to make an approximation to the ground state energy of a barrier system and we showed that it could be used to calculate the ground state level splitting for symmetric quartic potential. We then suggested a new numerical process for analyzing a path integral system and showed that it was able to reproduce the known analytic results of the symmetric potential.

It was then explained how the results of the calculation changed for a non symmetric potential. The appearance of an imaginary part to the ground state energy indicated that the local minimum state could not exist indefinitely. This imaginary part was related to the rate of decay away from the metastable side of the potential. It was then suggested that the formalism could be used to investigate a system that could decay from a metastable state into more than one lower energy configuration. In particular we derived for the first time a pair of coupled second order differential equations that an instanton for our multiferroic system must satisfy. We then approximated the solution to these equations using the numerical technique of chapter 2.

While we were able to perform some preliminary investigation on the behavior of this metastable system time restraints prevented a much fuller analysis. In the future one could analyse the behaviour of the system under various choices system parameters in order to understand how the two tunnelling rates are effected. Further more one could easily modify the potential to include other forms of coupling, other

forms of defect or a system where perhaps both domain walls were driven by fields of different strengths.

However there are difficulties with using this numerical method. The first of which is the slow rate of convergence of the algorithm. While in the one dimensional case the monte Carlo algorithm used to smooth the was reasonable quick to converge, this is not the case for our two dimensional problem. Initially converging quickly the algorithm was able to reduce the value of the objective function by around three orders of magnitude, however, from this point convergence becomes very slow. Unfortunately, this caused difficulty in calculating the prefactor. While the quantum Boltzman factor is determined directly form the instaton the prefactor requires knowledge of the derivative of the instaton which is more adversely effected by a lack of smoothness. The prefactor is also determined by considering a large τ extrapolation from the derivative making it particularly sensitive to small perturbations of the solution. Secondly the instatons calculated appear to over shoot the equipotential slightly, this can be seen in figure (5.4), an explanation for this is lacking but its effect is small. Some success in correcting this effect might come from decreasing the point spacing near the turning point of the instaton.

Despite this the method is still sufficiently accurate to investigate possible behaviors of a given system. It is conceivable that it might be useful as a guide when considering analytic approximations to similar problems. In particular one might use the numerical method to investigate the possible mechanisms for metastable decay and then decide which analytic approximations would be suitable for which mechanisms. While we were motivated be a metastable multiferroic system it is likely that there are many areas of physics where a system with competing decay mechanisms is of interest and the methods described here could also be of use in these areas.

References

- [1] Eugene M Chudnovsky and Javier Tejada. Macroscopic Quantum Tunneling of the Magnetic Moment.
- [2] Fetter and Walecka. Quantum theory of many particle systems. McGraw Hill, 1971.
- [3] R. P. Feynman. Space-time approach to non-relativistic quantum mechanics. Rev. Mod. Phys., 20(2):367–387, Apr 1948.
- [4] M. Fiebig, Th. Lottermoser, D. Frohlich, A. V. Goltsev, and R. V. Pisarev. Observation of coupled magnetic and electric domains. Letters to Nature, 2002.
- [5] Charles Fox. An introduction to the calculus of variations, chapter 1. Oxford University Press, 1950.
- [6] Peter Hänggi, Peter Talkner, and Michal Borkovec. Reaction-rate theory: fifty years after kramers. Rev. Mod. Phys., 62(2):251–341, Apr 1990.
- [7] N.A. Hill. Why are there so few magnetic ferroelectrics? J. Phys. Chem. B, 2000.
- [8] H. Jansson, G. Mills, and K. W. Jacobsen. Classical and Quantum Dynamics in Condensed Phase Simulations, chapter 16 - Nudged Elastic Band Method for Finding Minimum Energy Paths of Transitions. World Scientific, 1998.
- [9] Joo-Von Kin and R. L. Stamps. Hysteresis from antiferromagnet domain-wall processes in exchange bias systems: Magnetic defects and thermal effects. Physical Review B, 2005.
- [10] C. Kittel. Domain boundary motion in ferroelectric crystals and the dielectric constant at high frequency. Phys. Rev., 83(2):458, Jul 1951.
- [11] Charles Kittel. Introduction to Solid State Physics, chapter 15: Ferromagnetism and Antiferromagnetism, page 474. Wiley, 7 edition, 1953.

-
- [12] Hagen Kleinert. Path Integrals in Quantum Mechanics, Statistics and Polymer Physics.
- [13] J.S. Langer. Theory of the condensation point. Annals of Physics, 41(1):108–157, Jan 1967.
- [14] Lines and Glass. Principles and Applications of Ferroelectrics and Related Materials.
- [15] L. S. Shulman. Techniques and Applications of Path Integration.
- [16] Jian Zhai. Velocity of domain wall in ferromagnets with demagnetizing field. Physics Letters A, 2001.

Appendix A

Analytic Treatment of Double Well Potential

In this appendix we present the analytic treatment of the double well potential. This should explain a general technique of evaluating path integrals in the semi-classical (WKB) approach and providing a result for comparison with numerical results. There are many methods for evaluating specific stages of the calculation, the following presentation is a mixture between the presentation given by Kleinart [12] and Schulman [15] intended to insight into the numerical approximations.

A.1 General Explanation of Evaluation

We are interested in the analytically continued $t \rightarrow i\tau$ propagator

$$\langle x_f | e^{-\frac{\hat{H}\tau}{\hbar}} | x_i \rangle \quad (\text{A.1})$$

in particular the leading terms in large τ regime. So we wish to evaluate

$$\langle x_f | e^{-\frac{i\hat{H}t}{\hbar}} | x_i \rangle = \int \mathcal{D}[x(t)] e^{-\frac{iS}{\hbar}} \quad (\text{A.2})$$

with

$$S = \frac{m}{2} \int_0^t dt \left(\frac{d}{dt} x \right)^2 - V(x)$$

taking $t \rightarrow i\tau$ gives a new expression for the action

$$\begin{aligned} S &= \frac{m}{2} \int_{-\frac{\tau}{2}}^{\frac{\tau}{2}} \left(\frac{dt}{d\tau} \right) \left(\frac{d\tau}{dt} \frac{d}{d\tau} x \right)^2 - V(x) \\ &= -i \frac{m}{2} \int_{-\frac{\tau}{2}}^{\frac{\tau}{2}} d\tau i^2 \left(\frac{d}{d\tau} x \right)^2 - V(x) \end{aligned} \quad (\text{A.3})$$

and hence we have (with the tranformed action denoted S_e and referred to as the euclidean propagator)

$$\langle x_f | e^{-\frac{\hat{H}\tau}{\hbar}} | x_i \rangle = \int \mathcal{D}[x(\tau)] e^{-\frac{S_e}{\hbar}} \quad (\text{A.4})$$

with

$$S_e = \frac{m}{2} \int_{-\frac{\tau}{2}}^{\frac{\tau}{2}} d\tau \left(\frac{d}{d\tau} x \right)^2 + V(x)$$

As before we expand our paths in terms of weak variations around paths that are stationary with respect to the euclidean action. We assume currently that there is only one such path, this is of course no generally true but we can always sum the contributions from oth such stationary paths. We express any path $x(t)$ as a sum $x(t) = \bar{x}(\tau) + \Delta x(\tau)$ with $\bar{x}(\tau)$ the stationary point of the euclidean action (ie $\frac{\delta S_e[\bar{x}(\tau)]}{\delta x(\tau)} = 0$).

$$\begin{aligned} S_e[x(\tau)] & \quad (\text{A.5}) \\ &= S_e[\bar{x}(\tau) + \Delta x(\tau)] \\ &= S_e[\bar{x}(\tau)] + \int \frac{\delta S_e[\bar{x}(\tau)]}{\delta x(\tau)} \Delta x(t) d\tau \\ &+ \frac{1}{2!} \int \int \frac{\delta^2 S_e}{\delta x(\tau_1) \delta x(\tau_2)} \Delta x(t_1) \Delta x(t_2) d\tau_1 d\tau_2 + O\left(\frac{1}{3!} \Delta x(\tau)^3\right) \end{aligned}$$

Now the condition that the fist functional derivative be zero for $\bar{x}(\tau)$ implies that $\bar{x}(\tau)$ will obey the familiar Euler-Lagrange equations. The second functional derivative of the euclidean action is

$$\frac{\delta^2 S_e}{\delta x(\tau_1) \delta x(\tau_2)} = -m \left(\frac{d^2}{d\tau^2} \delta(\tau - \tau_2) \Big|_{\tau \rightarrow \tau_1} + \frac{d^2}{dx^2} V(x) \delta(\tau_1 - \tau_2) \right) \quad (\text{A.6})$$

So the second variation is

$$\begin{aligned} \delta^2 S_e &= \frac{1}{2!} \int \int \frac{\delta^2 S_e[\bar{x}(\tau)]}{\delta x(\tau_1) \delta x(\tau_2)} \Delta x(t_1) \Delta x(t_2) d\tau_1 d\tau_2 \quad (\text{A.7}) \\ &= \frac{m}{2!} \int \int \left(-\frac{d^2}{d\tau^2} \delta(\tau - \tau_2) \Big|_{\tau \rightarrow \tau_1} + \frac{d^2}{dx^2} V(x) \delta(\tau_1 - \tau_2) \right) \Delta x(t_1) \Delta x(t_2) d\tau_1 d\tau_2 \\ &\quad \text{performing one of teh integrals to collaps the delta function} \\ &= \frac{m}{2} \int -\Delta x(\tau_1) \Delta x''(\tau_1) + \frac{d^2}{dx^2} V(\bar{x}(\tau_1)) \Delta x(\tau_1)^2 d\tau_1 \end{aligned}$$

the negative of the above expression is usually denoted S_e^{fl} so if the series expansion is truncated after after the second order term we have

$$\begin{aligned} \langle x_f | e^{-\frac{\hat{H}\tau}{\hbar}} | x_i \rangle &= \int \mathcal{D}[x(\tau)] e^{-\frac{S_e[x(\tau)]}{\hbar}} \\ &= \int \mathcal{D}[\bar{x}(\tau) + \Delta x(\tau)] e^{-\frac{S_e[\bar{x}(\tau) + \Delta x(\tau)]}{\hbar}} \\ &\approx e^{S_e[\bar{x}(\tau)]} \int \mathcal{D}[\Delta x(\tau)] e^{-\frac{S_e^{fl}[\Delta x(\tau)]}{\hbar}} \end{aligned} \quad (\text{A.8})$$

we usually write

$$\approx e^{-\frac{S_e[\bar{x}(\tau)]}{\hbar}} \mathcal{F}$$

In doing so we have factored the problem into the contribution from the classical path and the contribution from quadratic fluctuations around that path (\mathcal{F}). The (\mathcal{F}) is much easier to deal with, it is now quadratic in the path variations with vanishing end points. To proceed the usual procedure will be to look for eigen values of

$$\left(-\frac{d^2}{d\tau^2} + V''[\bar{x}(\tau_1)]\right)y_n(\tau) = \lambda_n y_n(\tau) \quad (\text{A.9})$$

noting that this is of the Sturm-Liouville form

$$-\frac{d}{dx} \left[p(x) \frac{dy}{dx} \right] + q(x)y = \lambda w(x)y. \quad (\text{A.10})$$

Indicates that when properly normalised the y_n will form a total orthonormal basis for the lebesgue space $L^2\left[-\frac{T}{2}, \frac{T}{2}\right]$, $1dx$ and hence we can express our $\Delta x(\tau)$ in terms of an infinite sum of y_n

$$\Delta x(\tau) = \sum_{n=0}^{\infty} \zeta_n y_n(\tau) \quad (\text{A.11})$$

And so we can write

$$\begin{aligned} S_e^{fl} &= \frac{m}{2} \int \Delta x(\tau_1) \left(-\frac{d^2}{d\tau^2} + V''[\bar{x}(\tau_1)]\right) \Delta x(\tau_1) d\tau_1 \\ &= \frac{m}{2} \int \sum_{n=0}^{\infty} \zeta_n y_n(\tau) \left(-\frac{d^2}{d\tau^2} + V''[\bar{x}(\tau_1)]\right) \sum_{m=0}^{\infty} \zeta_m y_m(\tau) d\tau_1 \\ &= \frac{m}{2} \int \sum_{n=0}^{\infty} \zeta_n y_n(\tau) \sum_{m=0}^{\infty} \zeta_m y_m(\tau) \lambda_m d\tau_1 \\ &\quad \text{using the orthonormality of the } y_n \\ &= \frac{m}{2} \sum_{m=0}^{\infty} \zeta_m^2 \lambda_m \end{aligned} \quad (\text{A.12})$$

now in order to sum over all variations of the path it is necessary to integrate over all values of the ζ_m . In making this transformation to the basis of y_n we have

transformed the integration of paths into a infinite product of real valued integrals. Unfortunately the "Jacobian" of such a transformation is not easily defined but, as we shall see, it will not be necessary to determine the unknown constant that has been introduced.

$$\begin{aligned}
\mathcal{F} &= \int \mathcal{D}[\Delta x(\tau)] e^{\frac{-S_e^f[\Delta x(\tau)]}{\hbar}} \tag{A.13} \\
&= N \prod_{n=0}^{\infty} \left[\int_{-\infty}^{\infty} \frac{d\zeta_n}{2\pi\hbar} \right] \exp\left\{ \frac{-m}{2\hbar} \sum_{m=0}^{\infty} \zeta_m^2 \lambda_m \right\} \\
&= N \prod_{n=0}^{\infty} \int_{-\infty}^{\infty} \frac{d\zeta_n}{2\pi\hbar} \exp\left\{ \frac{-m}{2\hbar} \zeta_n^2 \lambda_n \right\} \\
&= \frac{N}{\sqrt{\prod_{n=0}^{\infty} \lambda_n}}
\end{aligned}$$

So the original path integral has now been reduced to

$$\langle x_f | e^{\frac{-\hat{H}\tau}{\hbar}} | x_i \rangle = e^{\frac{-S_e[\bar{x}(\tau)]}{\hbar}} \frac{N}{\sqrt{\prod_{n=0}^{\infty} \lambda_n}} \tag{A.14}$$

A.1.1 Evaluating the infinite product

In order to evaluate the infinite product given in equation A.13 it will be necessary to remove the normalisation N that was introduced when the path integral was transformed to a product of integrals over ζ_n to do this consider a solution $x_0(\tau)$ where the path remains constant this will be a stationary path with respect to the action, and its fluctuation term, call it \mathcal{F}_0 will have a fluctuation action of the form

$$\frac{m}{2} \int -\Delta x(\tau_1) \Delta x''(\tau_1) + \omega \Delta x(\tau_1)^2 d\tau_1 \tag{A.15}$$

with ω a constant. This is simply the fluctuation factor from a harmonic potential, which is exactly solvable. So we have

$$\begin{aligned}
\mathcal{F} &= \frac{N}{\sqrt{\prod_{n=0}^{\infty} \lambda_n}} \tag{A.16} \\
&= \frac{N}{\sqrt{\prod_{n=0}^{\infty} \lambda_n^0}} \frac{\sqrt{\prod_{n=0}^{\infty} \lambda_n^0}}{\sqrt{\prod_{n=0}^{\infty} \lambda_n}} \\
&= \mathcal{F}_0 \frac{\sqrt{\prod_{n=0}^{\infty} \lambda_n^0}}{\sqrt{\prod_{n=0}^{\infty} \lambda_n}}
\end{aligned}$$

where

$$\mathcal{F}_0 = \sqrt{\frac{\omega}{\pi\hbar}} e^{\frac{\omega\beta}{2\hbar}} \tag{A.17}$$

There is still a possible divergence in the above expression that shall be addressed in the section below

A.1.2 Zero Eigenvalue Solution

As the limits of the integration in the euclidean action tend to ∞ we expect that the soliton solution $x(\tau)$ to be translationly invariant. A instanton centered at τ_0 and another instanton infinitesimally separated at centered at τ'_0 will give the same contribution to our euclidean action. The difference between these solutions manifests it self as a fluctation around the instanton solution that does not change the euclidean action. As a consequence there will always exist an eigen function y_0 such that $y_0 = \alpha x'(\tau - \tau_0)$ and $\lambda_0 = 0$ the key to removing this divergence is to evaluate the contribution resulting from the invariance of a single instanton, replacing the integral over ζ_0 with an integral over the position the center of the instanton. It is possible to show that the α above is $\alpha = \sqrt{S_e[\bar{x}(\tau)]}$. Now our divergent contribution arises from the integral

$$\int_{-\infty}^{\infty} \frac{d\zeta_0}{\sqrt{2\pi\hbar}} \quad (\text{A.18})$$

recalling that

$$x(t) = \bar{x}(\tau_{-0}) + \Delta x(\tau) = \overline{x(\tau_{-0})} + \frac{m}{2} \sum_{m=0}^{\infty} \zeta_m^2 \lambda_m \quad (\text{A.19})$$

we have

$$\frac{dx}{d\zeta_0} = y_0 \quad (\text{A.20})$$

and

$$\frac{dx}{d\tau_0} = \bar{x}(\tau_{-0}) \quad (\text{A.21})$$

giving

$$\begin{aligned} x d\tau_0 &= y_0 d\zeta_0 \\ \Rightarrow d\zeta_0 &= \sqrt{S_e[\bar{x}(\tau)]} d\tau_0 \end{aligned} \quad (\text{A.22})$$

So we make the replacement

$$\frac{1}{\sqrt{\lambda_0}} = \sqrt{\frac{S_e[\bar{x}(\tau)]}{2\pi\hbar}} \int_{-\frac{L}{2}}^{\frac{L}{2}} d\tau_0 \quad (\text{A.23})$$

A.2 Specifics of Double Well potential

Thus far our anlysis has been a general motivation and definition , we now consider the specific example of the double well potential

$$V(x) = \frac{\omega^2}{8a^2} (x-2)^2 (x+2)^2 \quad (\text{A.24})$$

we have seen that (with the primes denoting total derivatives with respect to τ)

$$\begin{aligned} x'' - \frac{d}{dx}V(x) &= 0 & (A.25) \\ \Rightarrow x''x' - \frac{d}{dx}V(x)x' &= 0 \\ \Rightarrow \frac{d}{d\tau}\left(\frac{1}{2}x'^2 - V(x(\tau))\right) &= 0 \end{aligned}$$

in the limit of $\tau \rightarrow \text{inf}$ there are two solutions, the first is the trivial solution where the particle starts and remains at $\pm a$, the second non-trivial solution is

$$x(\tau) = \pm a \tanh \frac{\omega}{2}(\tau - \tau_0) \quad (A.26)$$

the $\tau - \tau_0$ being a reflection of the fact that in the $\tau \rightarrow \text{inf}$ limit the particle spends infinite time at its initial stationary point of the potential before crossing to the other stationary point where it remains indefinitely.

A.2.1 Classical Contribution to the Action

We can now easily evaluate the classical contribution to the action. In the case of the constant solutions we have $S_e[x(\tau) = \pm a] = 0$ however for the case of the non-trivial solution it is easily confirmed that

$$\int_{-\frac{\tau}{2}}^{\frac{\tau}{2}} d\tau \left(\frac{d}{d\tau} \pm a \tanh \frac{\omega}{2}(\tau - \tau_0) \right)^2 + V(\pm a \tanh \frac{\omega}{2}(\tau - \tau_0)) = \frac{2}{3}a^3\omega \quad (A.27)$$

A.2.2 Fluctuation contribution to Feynman Kernel

We must now evaluate the contribution to the propagator from the quadratic fluctuations around the action as we seek to diagonalize the fluctuation integral in order to reduce our problem to an infinite product of eigenvalues, as such we look for eigenvalues of the equation

$$\left(-\frac{d^2}{d\tau^2} + \omega^2 \left(1 - \frac{3}{2 \cosh^2(\omega \frac{\tau - \tau_0}{2})} \right) \right) y_n(\tau) = \lambda_n y_n(\tau) \quad (A.28)$$

At this point we are left with the problem of evaluating this infinite product. There are two problems to be encountered here the first is that we expect one of these eigenvalues to be zero, and the second is that we expect only a finite number of discrete eigenvalues before a continuum of solutions that will contribute to the product.

A.3 Discrete Eigen Value Contribution

While the exact solutions to the potential are available analytically here we will give only the result. The analytic technique used is known as the Duru-Kleinert

transformation and is detailed in Kleinert's book [12]. The transformation gives the eigenfunction solutions in terms of hyper-geometric functions. In the case of our potential they can be simplified to

$$y_0 = \sqrt{\frac{3\omega}{8}} \frac{1}{\cosh^2\left(\frac{\omega(\tau-\tau_0)}{2}\right)} \quad (\text{A.29})$$

and

$$y_1 = \sqrt{\frac{3\omega}{4}} \frac{\sinh\left(\frac{\omega(\tau-\tau_0)}{2}\right)}{\cosh^2\left(\frac{\omega(\tau-\tau_0)}{2}\right)} \quad (\text{A.30})$$

A.4 Continuum Eigenvalue Contribution

To proceed consider the form of our fluctuation contribution to the action and write it in terms of discrete positions using the standard definition of the integral, we see that we could write our expression in terms of a matrix

$$\begin{aligned} S_e^{fl} &= \frac{m}{2} \int \Delta x(\tau) \left(-\frac{d^2}{d\tau^2} + \omega^2 \left(1 - \frac{3}{2 \cosh^2\left(\omega \frac{\tau-\tau_0}{2}\right)} \right) \right) \Delta x(\tau) d\tau \quad (\text{A.31}) \\ &= \lim_{N \rightarrow \infty} \sum_{j=0}^N \Delta\tau \Delta x(\tau_j) [-\nabla \bar{\nabla} + V(x_i)] \Delta x(\tau_j) \\ &= \lim_{N \rightarrow \infty} \eta^T \underline{\sigma} \eta \end{aligned}$$

where

$$\eta = \begin{bmatrix} \Delta x(\tau_0) \\ \Delta x(\tau_1) \\ \cdot \\ \cdot \\ \cdot \\ \Delta x(\tau_N) \end{bmatrix}$$

and

Now using the definition of the path integral [12] we can write

$$\int \mathcal{D}[\Delta x(\tau)] e^{-\frac{S_e^{fl}[\Delta x(\tau)]}{\hbar}} = \lim_{N \rightarrow \infty} \left(\frac{m}{2\pi\hbar\Delta\tau} \right)^{\frac{N+1}{2}} \int d^N \eta e^{\eta^T \underline{\sigma} \eta} \quad (\text{A.33})$$

Now since all the entries of $\underline{\sigma}$ are real there will exist a unitary matrix \underline{U} which can be used to diagonalise $\underline{\sigma}$:

$$\underline{\sigma} = \underline{U}^\dagger \underline{\sigma}_D \underline{U} \quad (\text{A.34})$$

this allows A.33 to be written as

$$\lim_{N \rightarrow \infty} \left(\frac{m}{2\pi\hbar\Delta\tau} \right)^{\frac{N+1}{2}} \int d^N \eta e^{\eta^T \underline{\sigma} \eta} = \lim_{N \rightarrow \infty} \left(\frac{m}{2\pi\hbar\Delta\tau} \right)^{\frac{N+1}{2}} \int d^N \eta' e^{\eta'^T \underline{\sigma}_D \eta'} \quad (\text{A.35})$$

with $\eta' = \underline{U}\eta$. Now if we take a large N approximation we can perform our integration as a product of gaussian integrals. Giving us

$$\begin{aligned} \int \mathcal{D}[\Delta x(\tau)] e^{-\frac{S_e^{fl}[\Delta x(\tau)]}{\hbar}} &\approx \left[\left(\frac{m}{2\pi\hbar\Delta\tau} \right)^{N+1} \frac{\pi^N}{\det \underline{\sigma}_D} \right]^{\frac{1}{2}} \\ &= \left[\left(\frac{m}{2\pi\hbar\Delta\tau} \right)^{N+1} \frac{\pi^N}{\det \underline{U}^\dagger \underline{\sigma}_D \underline{U}} \right]^{\frac{1}{2}} \end{aligned} \quad (\text{A.36})$$

since $\det \underline{U} = 1$

$$\begin{aligned} &= \left[\left(\frac{m}{2\pi\hbar\Delta\tau} \right)^{N+1} \frac{\pi^N}{\det \underline{\sigma}} \right]^{\frac{1}{2}} \\ &= \left[\left(\frac{m}{2\pi\hbar\Delta\tau} \right) \frac{1}{\left(\frac{2\hbar\Delta\tau}{m} \right)^N \det \underline{\sigma}} \right]^{\frac{1}{2}} \end{aligned}$$

And hence all that remains is to evaluate the determinant of

$$\left(\frac{2\hbar\Delta\tau}{m} \right)^N \det \underline{\sigma} = \begin{vmatrix} 2 + \Delta\tau^2 V[x_1] & -1 & & & \\ -1 & 2 + \Delta\tau^2 V[x_2] & -1 & & \\ & -1 & 2 + \Delta\tau^2 V[x_3] & -1 & \\ & & & \dots & \\ & & & & \dots \end{vmatrix}$$

in order to evaluate this determinant we could consider first the determinant of the M sub matrices S_M where S_M is the matrix contained in the upper left hand corner

of the matrix in A.37 with the ultimate goal of evaluating $\det S_N$. By considering the determinants of these matrices we can define the recursive relationship

$$|S_M| = \left(2 - \frac{\Delta\tau^2}{m} V[x_M] \right) |S_{M-1}| - |S_{M-2}| \quad (\text{A.37})$$

where $|S_1| = 2 - \frac{\Delta\tau^2}{m} V[x_1]$ is the trivial determinant of the 1×1 matrix contained in the upper left corner. For consistency we must let $|S_0| = 1$. If in the above recursive relation we group all the terms that are only dependent on the discrete time spacing and equate them with terms that contain an explicit dependence on the mass and potential we obtain the following,

$$\frac{|S_{M+1}| - |S_M| + |S_{M-1}|}{\Delta\tau^2} = -\frac{V[x_{M+1}]|S_M|}{m} \quad (\text{A.38})$$

which has the form of a discrete approximation of a second order differential equation. As we take the limit of $\Delta\tau^2 \rightarrow \infty$ the submatrices $|S_{M+1}|$ and $|S_{M-1}|$ will approach $|S_M|$ and will have a differential equation of the form

$$\frac{\partial^2 f(\tau, \tau_i)}{\partial\tau^2} = \frac{V(x(\tau))}{m} f(\tau, \tau_i) \quad (\text{A.39})$$

with the boundary conditions $f(0, \tau_i) = 0$ and $\frac{\partial f(0, \tau_i)}{\partial\tau} = 1$. Our determinant will be obtained by finding the value of the function at $f(\tau_i)$.

Having determined the classical path and hence the contributions from this path and the discrete eigenvalues in the expansion all that remains is the determination of the product of continuum eigen value solutions. From [15] we know that the product can be written in terms of the ratio of solutions to two differential equations.

$$\frac{1}{2} \frac{d^2 f(\tau)}{d\tau^2} = -\frac{1}{2} V''[\bar{x}(\tau)] \frac{f(\tau)}{m} \quad (\text{A.40})$$

and

$$\frac{d^2 f^0(\tau)}{d\tau^2} = -\omega^2 \frac{f^0(\tau)}{m} \quad (\text{A.41})$$

where ω^2 was obtained by considering the contribution from the degenerate instanton solution. We are interested in evaluating the object

$$R^2 = \frac{f^0(\beta)\lambda_1\lambda_0}{f(\beta)} \quad (\text{A.42})$$

Both with the boundary condition

$$\begin{aligned} f(0) &= 0 \\ \frac{df(0)}{d\tau} &= 1 \end{aligned} \quad (\text{A.43})$$

Since β will be large in the small temperature limit we can easily approximate the differential equation related to the degenerate solution with [15]

$$f^0(\beta) \approx \frac{1}{2\omega} e^{\beta\omega} \quad (\text{A.44})$$

This leaves only the first equation. The derivative of the stationary solution (the eigenfunction corresponding to the zero eigen value solution) will satisfy A.40 but will fail to satisfy the boundary conditions. There must, however, exist a second linearly independent solution such that the two can be combined to satisfy the boundary conditions.

$$f(\tau) = c_1 f_1(\tau) + c_2 f_2(\tau) \quad (\text{A.45})$$

Recall that the instanton will be well localised in the large temperature limit and that the first derivative of the potential should disappear near the end points. Hence the two solutions will be $\exp(\pm\kappa x)$ in the large x limit. It is clear that the exponentially decaying solution will correspond to the zero eigen value mode. We can therefore approximate the exponential by matching it to the decaying tail of the numerically determined zero solution. Having now approximated the asymptotic behavior of one solution we can easily approximate the other. In order that the second solution be linearly independent we require that the wronskian of the two solutions be non zero. We have already argued that the form of the solutions should be exponential (and hence the wronskian constant) we let the wronskian be equal to one

$$f_1 f_2' - f_2 f_1' = 1 \quad (\text{A.46})$$

Combining this with the boundary conditions we obtain $c_1 = -f_2(0)$ and $c_2 = f_1(0)$ one can show that $f(\beta) = \frac{1}{\kappa}$. The remaining two discrete eigenvalues are all that remain to be evaluated. The nonzero eigen values will already have been determined. The only remaining problem is that one of our eigen values has so far been treated as zero. However in the small but non zero temperature limit the imaginary time translational invariance will not be infinite. We expect then that the zero eigen value will not quite be zero. To make an approximation to the size of this small eigenvalue we consider equation A.8 and let $(-\frac{d^2}{d\tau^2} + V''[\bar{x}(\tau_1)])y(x) \rightarrow Hy(x)$

$$Hy(x) + \lambda_0 y(x) = 0 \quad (\text{A.47})$$

with $y(0) = y(\beta) = 0$. We can then write equation A.47 as an integral equation. We let $HG(x, z) = \delta(x - z)$ and $H\Psi = 0$ and we have

$$y(x) = \Psi(x) - \lambda_0 \int_0^\beta G(x, z)y(z)dz \quad (\text{A.48})$$

We can solve for Ψ and G in terms of functions f_1 and f_2 and take the first born approximation to equation A.48. The final result can shown to be $\lambda_0 \approx \frac{f_1(\beta)}{f_2(\beta)}$ And hence we have all the information we need to make an approximation to the contribution to the imaginary time propagator from a single kink instaton solution

A.5 Rare Gas of Instatons

Combing the various results above we have

$$\langle \pm a | e^{-\frac{\hat{H}\tau}{\hbar}} | \mp a \rangle \approx e^{-\frac{S_e[\bar{x}(\tau)]}{\hbar}} \mathcal{F}_0 K' \sqrt{\frac{S_e[\bar{x}(\tau)]}{2\pi\hbar}} \int_{-\frac{\tau}{2}}^{\frac{\tau}{2}} d\tau_0 \quad (\text{A.49})$$

Where we have defined

$$K' = \frac{\sqrt{\prod_{n=0}^{\infty} \lambda_n^0}}{\sqrt{\prod_{n \neq 0}^{\infty} \lambda_n}} \quad (\text{A.50})$$

Thus far considered only one stationary solution to the action. There does however exist numerous solutions. In the limit of zero temperature there will in fact be an infinite number of solutions. We must consider solutions that cross the barrier region multiple times and their contribution to the transformed propagator. We now have two classes of solutions those that cross the barrier an odd number of times and finish in the other side of the barrier and those that cross an even number of times to return to the initial well. Recalling the well localised form of the single kink solution, we assume that a solution can be approximated by the piece wise connection of N single solutions where we alternate between $\pm x(\tau)$, see figures ????. We assume that the distance from the center of one solution to the center of the next, $\Delta\tau$ say, is much larger than the characteristic width of the instaton solution. In this approximation a solution consists of multiple transitions from one well to the other happens with each transition from those preceding it. Noting that the approximately stationary sections of the stationary path, ie far away from a kink contribute little to the action (since they correspond to regions of negligible kinetic and potential energy in the imaginary phase space) We can write the contribution to the euclidean action $S_{e,N}$ as

$$S_{e,N} = N S_e[\bar{x}(\tau)] \quad (\text{A.51})$$

We expect that contribution from the zero eigenvalue mode will still enter into our calculation. The Jacobian factor associated with each instaton will remain unchanged.

$$\sqrt{\frac{S_e[\bar{x}(\tau)]}{2\pi\hbar}}^N \quad (\text{A.52})$$

However the integral associated with the degrees of freedom of the placement of the instaton will be reduced for each additional inston. If we index the placement of the instatons starting from $\infty \rightarrow -\infty$ and label the positions of their ceters by τ_i we see that the first instaton retains the term

$$\int_{-\frac{L}{2}}^{\frac{L}{2}} d\tau_0 \quad (\text{A.53})$$

When considering the postion of the next instaton we must be careful to avoid counting its contribution multiple times. An interchange of the positions of two of the solutions is not a new solution. Each subsequent instaton will be positioned a imaginary time greater than all preceeding instatons (ie $\tau_i > \tau_{i-1}$). The contribution for the second instaton should be

$$\int_{-\frac{L}{2}}^{\tau_0} d\tau_1$$

and in general

$$\int_{-\frac{L}{2}}^{\frac{L}{2}} d\tau_0 \int_{-\frac{L}{2}}^{\tau_0} d\tau_1 \int_{-\frac{L}{2}}^{\tau_1} d\tau_2 \dots \int_{-\frac{L}{2}}^{\tau_{N-1}} d\tau_N = \frac{L^N}{N!} \quad (\text{A.54})$$

We must now consider the contribution from the the eigenvalue products. Note that the eigenvalues that we need will no longer be solved on the interval $(-\frac{L}{2}, \frac{L}{2})$ but rather the sub-intervals (τ_{i-1}, τ_i) giving the contribution.

$$\prod_{i=1}^N \frac{1}{\sqrt{\prod_{n=0}^{\infty} \lambda_n}} \Big|_{(\tau_{i-1}, \tau_i)} \quad (\text{A.55})$$

We have approxamated our solution by a smooth peice wise sum of kinks. The single kink solution on the interval (τ_{i-1}, τ_i) will not have reached $\pm a$. It is possible to show for N kinks this introduces the additional factor.

$$\sqrt{\frac{\omega}{\pi \hbar}}^{-(N-1)} \quad (\text{A.56})$$

The details are some what technical and shall not be presented here. The argument involves introducing additional factors related to the fact that when finding a basis for our x we will not have the zero boudary condition. We have had to assume here that the the end points are close to $\pm a$ so that the bottom of the potential can be approxamated by a harmonic potential, hence the prior assumption of non interacting solutions.

As before we will expand around the stationary path. When evaluating the fluctuation factor we could express the integral $S_e^{\text{fl}}[\Delta x] = S_e[x + x]$ as sum of integrals

over the intervals $[\tau_i, \tau_{i+1}]$. Recalling that previously we multiplied our product of eigen values by the known solution from the degenerate instaton in order to remove an unknown constant. Referring to equations A.17 A.55 A.56, we have for our ratio of eigen values

$$\sqrt{\frac{\omega}{\pi\hbar}}^{-(N-2)} e^{\frac{\omega\beta}{2\hbar}} \sqrt{\prod_{n=0}^{\infty} \lambda_n^0}_{(\tau_0, \tau_N)} \prod_{i=1}^N \frac{1}{\sqrt{\prod_{n=0}^{\infty} \lambda_n}_{(\tau_{i-1}, \tau_i)}} \quad (\text{A.57})$$

We note that we could decompose the eigenvalue product due to the degenerate solution exactly as we have the product due to the multiple kink solution giving

$$\sqrt{\frac{\omega}{\pi\hbar}} e^{\frac{\omega\beta}{2\hbar}} \prod_{i=1}^N \frac{\sqrt{\prod_{n=0}^{\infty} \lambda_n^0}_{(\tau_{i-1}, \tau_i)}}{\sqrt{\prod_{n=0}^{\infty} \lambda_n}_{(\tau_{i-1}, \tau_i)}} \quad (\text{A.58})$$

The ratio of eigen value ratios corresponds now to the contribution from a single eigen value solution K' . So for the N kink solution we have

$$\langle \pm a | e^{-\frac{\hat{H}\tau}{\hbar}} | \mp a \rangle_{N \text{ kinks}} = e^{-\frac{NS_e[\bar{x}(\tau)]}{\hbar}} \mathcal{F}_0 K'^N \sqrt{\frac{S_e[\bar{x}(\tau)]}{2\pi\hbar}}^N \frac{\beta^N}{N!} \quad (\text{A.59})$$

Recalling that $\sum_{\text{odd}} \frac{x^n}{n!} = \sinh(x)$ and $\sum_{\text{even}} \frac{x^n}{n!} = \cosh(x)$ if we sum together or the odd or even solutions we have

$$\langle \pm a | e^{-\frac{\hat{H}\tau}{\hbar}} | a \rangle = \sqrt{\frac{\omega}{\pi\hbar}} e^{-\frac{\omega\beta}{2\hbar}} \beta \times \frac{1}{2} \left[\exp\left(K\beta e^{-\frac{S_e[x(\tau)]}{\hbar}}\right) \pm \exp\left(-K\beta e^{-\frac{S_e[x(\tau)]}{\hbar}}\right) \right] \quad (\text{A.60})$$

List of Figures

1.1	Electric and Magnetic Domain walls	2
2.1	A simple schematic showing two possible paths that a point particle might take from A to C	5
2.2	A potential with a meta-stable state	8
2.3	The Symmetric double well	15
2.4	One kink and Two kink solutions	17
3.1	Monte Carlo for smoothing solutions	21
3.2	Numerically determined solutions to 2.24	23
4.1	Zero Eigenvalue Mode	27
4.2	Zero Eigenvalue Mode	27
5.1	The form of the coupling energy	33
5.2	Two Solitons	35
5.3	Monte Carlo for smoothing solutions	36
5.4	Log plots of the tunnelling rates of the two possible solutions	37
5.5	Monte Carlo for smoothing solutions	38